STUDIES IN THE APPLICATION OF A REAL TIME COMPUTER TO ELECTROCHEMISTRY

A THESIS

Presented to

The Faculty of the Division of Graduate Studies

By

Alan Conrad Hayman

In Partial Fulfillment

of the Requirements for the Degree

Doctor of Philosophy

in the School of Chemistry

Georgia Institute of Technology

October, 1976

STUDIES IN THE APPLICATION

OF A REAL TIME COMPUTER

TO ELECTROCHEMISTRY

Approved:

Dr. Peter E. Sturrock, Chairman

Dr. Henry M. Neuman

Dr. Richard F. Browner

Date approved by Chairman 22 Nov 76

ACKNOWLEDGMENTS

I would like to acknowledge with the greatest of pleasure the unselfish assistance of Dr. Peter E. Sturrock, who is both friend and professor. I have enjoyed, and am deeply grateful for, the association that I have enjoyed with him in the last few years. Dr. Peter Sherry, Dr. Henry Neuman, and Dr. Richard Browner all made significant contributions in the writing of this thesis. Their help is gratefully acknowledged.

This work was supported by a Teaching Assistantship provided by the School of Chemistry. I want to thank the former Director, Dr. William M. Spicer, and the current Director, Dr. J. Aaron Bertrand, for this assistance. I would also like to thank Dr. H. A. Flaschka for introducing me to other areas of analytical chemistry which I appreciate much more now than I did at the time.

In conclusion, I thank my wife, Katherine, for her support, understanding, and acceptance during these hard years in graduate school. Without her I might not have finished. Many thanks to my father and mother who raised me, taught me, and gave me my moral values.

TABLE OF CONTENTS

TABLE OF CONTENTS (Continued)

LIST OF TABLES

LIST OF ILLUSTRATIONS

SUMMARY

Many variations are possible within square-wave polarography. However, most instruments are designed without sufficient flexibility in number and frequency of square pulses, pulse size, sampling times, etc. The purpose of this study was to experimentally evaluate the importance of such variables and to establish optimum values for the design of future instruments.

This study required an instrument with great flexibility in the timing of potential changes and current measurements. It also required numerical analysis of noise levels and base lines. These requirements dictated the use of an instrument in which the timing and data analysis functions are handled by a digital computer.

A previously constructed potentiostat was modified for the study and interfaced to a PDP-8e laboratory computer. A foreground-background program for the control of the instrument and data acquisition and analysis was written in PDP-8e assembly language. With this program, the values of experimental parameters can be entered via Teletype prior to each experimental run and the results printed by the Teletype and plotted on an XY recorder.

The experiments performed in this study indicate that the optimum delay between pulse application and current sampling is on the order of one millisecond rather than the forty milliseconds used in commercial instruments. The effectiveness of a positive feedback loop in decreasing pulse capacitance current was clearly indicated. It was also found that

the signal-to-noise ratio increased with both the number of data points taken for each pulse and the number of square pulses applied per drop.

CHAPTER I

THEORY

Classical (DC) Polarography

Polarography is an electrochemical technique in which potential is applied to a small electrode and the resulting cell current measured. As a potential is reached at which an electron transfer reaction can occur, the cell current increases. The increase in current is limited by the rate at which the reactant can diffuse to the electrode surface and hence is proportional to the concentration of the reacting species in the bulk of the solution. Further increases in potential do not yield further increases in current until a potential is reached at which another electron transfer reaction can occur. The result of a polarographic experiment, called a polarogram, is a display of cell current on the ordinate and electrode potential on the abscissa. The potential at which a current increase, or wave, occurs is used to identify the particular electron transfer reaction, and the amount of current increase in the wave is used to determine the concentration of reactant.

The potential at which the current has increased to one half of its maximum for a wave, is called the half-wave potential, $E_{\frac{1}{2}}$. The shape of the polarographic wave is given by:

$$E = E_{\frac{1}{2}} + (RT/nF)\ \mathrm{Ln}((i_d - i)/i) \qquad (1)$$

where

$$E_{\frac{1}{2}} = E_o - (RT/nF)\ \mathrm{Ln}(D_o/D_r)^{\frac{1}{2}} \quad .$$

Equation 1 results from the combination of the diffusion equations for the electrode process with the Nerst equation. In equation 1, R is the gas constant, T the absolute temperature, F the Faraday, n the number of electrons transferred in the half-reaction equation, and i the current increase at any point on the rising portion of the wave. D_o and D_r are the diffusion coefficients for the oxidized and reduced species in the half reaction.

Early attempts to utilize diffusion controlled processes for analysis led to erratic results because of day to day changes in the condition of the electrode surface. Heyrovsky[1] introduced the use of the dropping mercury electrode (DME) which gives reproducible results because the mercury drop is periodically replaced, thus giving a fresh, uncontaminated surface at which the reaction can occur.

The DME consists of a length of fine bore capillary tubing connected at one end to a reservoir of mercury. The other end of the capillary tubing dips into the cell solution. Mercury from the reservoir flows slowly through the capillary forming a drop electrode at the solution end. This drop grows slowly until it falls and is replaced by a new growing drop. It is now common practice to dislodge the drop at a preset time by striking the capillary with the armature of a solenoid. This eliminates variations in the drop time that result from changes in the mercury-solution interfacial tension as the electrode potential is changed.

Starting from the Cottrell equation (see Equation 5), which in turn is based on Fick's laws of diffusion, Ilkovic[2] derived the theoretical equation relating diffusion limited current at the DME to concentration:

$$i_d = 702nD^{1/2}Cm^{2/3}t_d^{1/6} \qquad (2)$$

In Equation 2, t_d is the time (sec) between detachments of successive electrode drops (referred to hereafter as drop time). C is the concentration of reactant (mmoles/l), m is the flow rate of mercury (mg/sec), and D is the diffusion coefficient (cm^2/sec).

The current varies as the electrode drop grows and is detached. The i_d of Equation 2 is the instantaneous current (microamperes) at the end of the drop life. Often, variations in the cell current are damped electrically, and in this case, the average current recorded is 6/7 of the maximum instantaneous current given by Equation 2.

Equation 2 was derived with the assumption that diffusion was the only process by which reactant was transported from the bulk of the solution to the electrode surface. In order to approximate this condition experimentally, it is necessary to add an inert salt (supporting electrolyte) to the cell solution. This supporting electrolyte minimizes transport of the reactant by electrical migration and also serves to decrease the ohmic resistance of the solution.

Limitations of DC Polarography

If the electron transfer current (DC-Faradaic current) discussed above were the only source of current in the cell, it should be possible to amplify it electronically and achieve almost limitless sensitivity.

However, there is another source of current in the cell which is independent of reactant concentration and acts to limit the sensitivity of DC Polarography. This other current is called the capacitance current or charging current. It arises from the fact that the interface between the mercury drop and the cell solution acts as a capacitor.

This capacitor requires current to charge the electrode to the desired potential. As the electrode drop grows, the surface area increases, the capacitance increases, and a continual flow of current is needed to keep the electrode at the desired potential. Furthermore, the capacitance is not a linear function of the electrode potential so the capacitance current varies as the potential is changed during the recording of a polarogram. In practice, the magnitude of the capacitance current is such as to obscure the Faradaic current when the concentration of reactant is significantly less than 10^{-5} moles per liter.

A second limitation of DC Polarography is evident in solutions of more than one reactant species. If the species that reacts first, as the electrode potential is varied, is of equal or lower concentration than the species that reacts second, no particular problem exists. However, if the second species is much lower in concentration than the first species, it is very difficult to accurately measure the diffusion current due to the second species. For example, 10^{-5} molar Cd(II) can be determined with reasonable accuracy if present alone in the solution. However, in the presence of 10^{-3} molar Pb(II), 10^{-5} molar Cd(II) is almost undetectable by DC Polarography.

Modern Variants of Polarography

A number of variations of polarography have been developed in attempts to overcome the limitations discussed above and, in some cases, to reduce the time required for obtaining a polarogram.

In one variation, the cell current is measured only at a time just prior to drop detachment. This technique is known as Tast polarography and serves to improve the ratio of DC-Faradaic current to the capacitance (DC) current. At any fixed potential, the DC capacitance current is given by:

$$i_c = (dA/dt)q = Km^{1/3}\bar{t}^{1/3}q \qquad (3)$$

where q is the integral double-layer capacitance, A is the surface area of the electrode, K is a constant, and m and t have the same significance as in Equation 2. From Equation 3 it can be seen that i_c decreases with time and will be a minimum at the end of the drop life. On the other hand, the DC-Faradaic current increases with time so that the ratio of Faradaic to capacitance current is greatest at the end of the drop. However, for reasonable drop times, the improvement in this ratio over the averaged values usually recorded is only about a factor of two[3].

Another variation of polarography is derivative-DC polarography. In this technique, cell current is differentiated electronically and dI/dE plotted versus E. Before the differentiation can be performed, it is necessary to filter out the current fluctuations due to the growth and detachment of the electrode drops. The derivative presentation results in a peak for each polarographic process rather than the steps observed on a DC polarogram. The potential of the peak corresponds

to the conventional $E_{\frac{1}{2}}$ and the peak current is proportional to concentration. This technique simplifies the analysis of multicomponent solutions and also has some increase in sensitivity over DC polarography. However, nothing is done to separate the capacitance and Faradaic currents so that the increase in sensitivity over DC polarography is not large.

AC polarography also results in a derivative-like readout. However, the process is quite different from derivative-DC polarography. A small AC voltage signal (usually < 25mV, peak to peak) is superimposed on the usual DC electrode potential. The resulting AC component of the total cell current is measured and recorded. The AC current is greatest when the DC current is changing the most rapidly.

An additional benefit can be obtained with AC polarography. The phase relationship between the applied AC voltage and the measured AC current is different for capacitance current and Faradaic current. Thus by using a phase-selective detector to measure the AC current, a partial separation can be achieved between the desired AC-Faradaic current and the undesired AC-capacitance current. However, the phase relationship between the applied AC voltage and the measured AC-capacitance current is a function of the product of the cell resistance and electrode capacitance. These two parameters change with time as the electrode drop grows to that the optimum rejection of the capacitance current can be achieved at only one point in the life of each drop. This optimum point varies as the double-layer capacitance varies with electrode potential.

An alternate method for separating the capacitance and Faradaic currents is based on their different decay rates following the application of a potential step. This is the basis for square-wave and pulse polarography which is the central topic of this work.

Square-Wave Polarography

When the potential of an electrode is changed abruptly by the application of a pulse, capacitance current flows until the electrode is charged to the new potential. The current flow is large at first and rapidly decays in accordance with Equation 4 (see Figure 1 a,c):

$$i_c = (\Delta E/r)\exp(-t/rc) \qquad (4)$$

In Equation 4, r is the cell resistance, c is the differential double-layer capacitance, t is the time after pulse application, and ΔE is the magnitude of the potential step. If the potential step is relaxed (i.e. stepped back), capacitance current flows in the opposite direction. From Equation 4 it can be seen that the smaller the product, rc, the more quickly the pulse-capacitance current decays. In an electrochemical cell, the higher the concentration of supporting electrolyte the lower the resistance and the more quickly the pulse-capacitance current decays.

If the potential change discussed above takes the electrode to a potential at which an electrode reaction occurs, a pulse-Faradaic current will also flow. Under linear diffusion-controlled conditions, the pulse-Faradaic current is given by:

$$i_F = nFACD^{\frac{1}{2}}/\pi^{\frac{1}{2}}t^{\frac{1}{2}} \qquad (5)$$

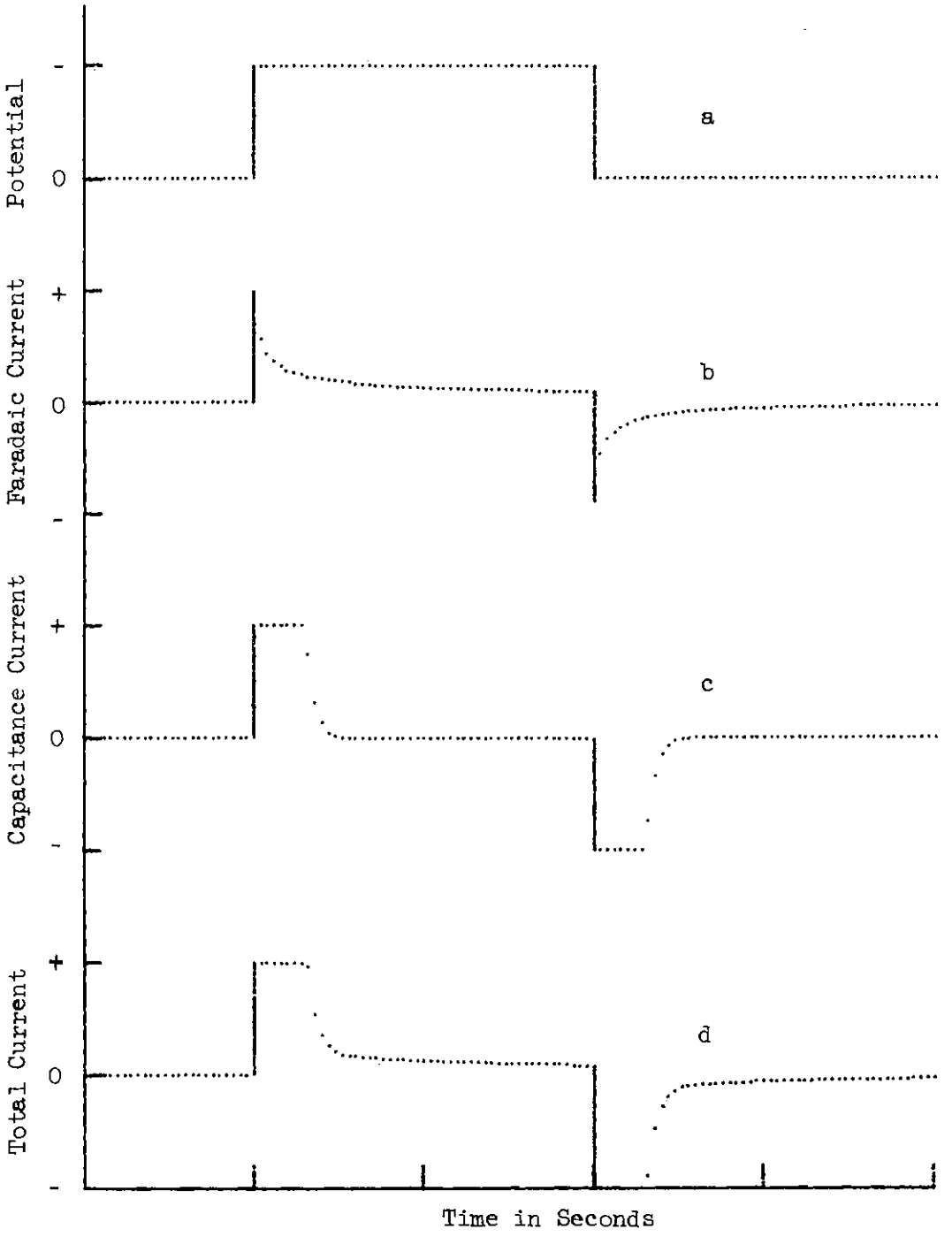

Figure 1. Potential Step and Resulting Currents.

where n, F, D, and t were defined above, A is the electrode surface area, and C is the reactant concentration.

A theoretical pulse-Faradaic current curve, based on Equation 5, is shown in Figure 1b. It can be seen that the pulse-Faradaic current does not decay as rapidly as the pulse-capacitance current. Figure 1d shows the total pulse current (capacitance + Faradaic). It can be seen that after some time delay, the pulse-capacitance current becomes negligible as compared to the pulse-Faradaic current. At that time, the total pulse current is essentially equal to the pulse-Faradaic current. If the current is sampled at that time, an almost complete rejection of the undesired pulse-capacitance current is achieved.

The rejection of the pulse-capacitance current, as described above, is the salient feature of square-wave polarography. In square-wave polarography, a small amplitude (usually < 50 mV) square wave is superimposed on the usual DC electrode potential. The DC electrode potential is slowly changed so as to scan the potential region for the polarogram. Current is sampled after a sufficiently long time delay to allow the pulse-capacitance current to decay adequately. Pulse-Faradaic current is plotted versus DC potential, and the polarogram has the same "derivative" form as those obtained by derivative-DC polarography and AC polarography.

Theoretical Equations for Square-Wave Polarography

Square-wave polarography was first reported by Barker and Jenkins[4]. The theoretical equation for the pulse-Faradaic current in square-wave polarography was derived by Barker[5]. The following discussion follows Barker's derivation.

For a reduction reaction, Equation 2 can be rewritten:

$$i_d = KC_o \tag{6}$$

where

$$K = 702nDm^{2/3}t_d^{1/6} .$$

For potentials at which the process is not diffusion limited:

$$i = K(C_o - C_o^o) \tag{7}$$

where C_o^o is the concentration of the oxidized form at the surface of the electrode and C_o is that in the bulk of the solution. The reduced form is produced by the electrode reaction and has a surface concentration,

$$C_r^o = i/K' \tag{8}$$

where K' differs from K only in the numerical value of the diffusion coefficient. Combining Equations 7 and 8:

$$C_r^o = (C_o - C_o^o)K/K' \quad . \tag{9}$$

Combining Equation 9 with the Nernst equation:

$$E = E_{1/2} + (RT/nF)\ \mathrm{Ln}(C_o^o/(C_o - C_o^o)) \tag{10}$$

where $E_{1/2}$ is the same as in Equation 1.

In order to determine the change in C_o^o with changes in E, Equation 10 is solved for C_o^o and differentiated with respect to E. Rearranging Equation 10 into exponential form:

$$C_o^o/(C_o - C_o^o) = \exp((E - E_{1/2})nF/RT) = P \qquad (11)$$

and further rearrangement gives:

$$C_o^o = C_o P/(1 + P) \quad . \qquad (12)$$

Differentiating Equation 12 with respect to E:

$$dC_o^o/dE = (nF/RT)C_o P/(1 + P)^2 \quad . \qquad (13)$$

For a small amplitude square wave:

$$\Delta C_o^o = (nF/RT)C_o \Delta E P/(1 + P)^2 \quad . \qquad (14)$$

The number of moles of a diffusing substance that diffuse across a plane of unit area in the time, dt, is known as the flux. By analogy to a corresponding heat transfer problem, the flux of reactant at the surface, f_o^o is:

$$f_o^o = \Delta C_o^o (D/\pi)^{1/2} \sum_{m=0}^{\infty} (-1)^m/(m\tau + t)^{1/2} \qquad (15)$$

where m is the number of half cycles of the square wave at time t, and τ is the half-cycle time. The flux at the surface is also given by:

$$f_o^o = i/nFA \quad . \qquad (16)$$

Combining Equations 14 through 16 and defining $\beta = t/\tau$:

$$i = (n^2F^2/RT)AC_o \Delta E(P/(1 + P)^2)(D/\pi\tau)^{1/2} \sum_{m=0}^{\infty} (-1)^m/(m + \beta)^{1/2} \qquad (17)$$

In practice, the upper limit of the summation is determined by the life time of the DME drop. As Barker[5] pointed out, Equation 17 is approximate since no correction was made for the effect of the drop expanding into the diffusion layer and it is also limited to small values of ΔE.

As the DC potential is swept slowly during the recording of a square-wave polarogram, the value of P (see Equation 11) changes. When the potential equals the half-wave potential the term, $P/(1 + P)^2$, is at its maximum value and thus current is at its peak value. A square-wave polarogram is influenced by n in two ways. First, P contains n so that the width of the polarographic peak depends on n. At 25° the width of the peak at half the peak height (half-peak width) is 89.4/n millivolts. Second, the magnitude of the peak is proportional to n^2. Thus, reactions with a two electron transfer give polarographic peaks four times higher and with one half the half-peak width of those for one electron transfers.

Pulse polarography is a common variation of square-wave polarography in which only one pulse is applied to the electrode during the drop life. Considering only the current for the application (not including the relaxation) of one pulse, Equation 17 reduces to:

$$i = (n^2F^2/RT)AC_o\Delta E(P/(1 + P)^2)(D/\pi t)^{1/2} \qquad (18)$$

Parry and Osteryoung[6] derived a more general form of Equation 18 which is not restricted to small values of ΔE:

$$i = nFAC_o((P\delta^2 - P)/(\delta + P\delta^2 + P + P^2\delta))(D/\pi t)^{1/2} \qquad (19)$$

where

$$P = \exp((E_1 + E_2)/2 - E_{1/2})nF/RT$$

and

$$\delta = \exp((E_2 - E_1)/2)nF/RT \quad .$$

Table 1 contains a comparison of calculations based on Equations 18 and 19. Equation 19 predicts wider and lower peaks than Equation 18, and this difference increases rapidly as ΔE is increased.

The derivation of Parry and Osteryoung[6] is based on the theoretical current response to a single potential step and is not directly applicable to the multistep situation of square-wave polarography. However, experimental evidence[7] points to a similar peak distortion, with increasing ΔE, for square-wave polarography. Applying the shape factor derived by Parry and Osteryoung[6] to Equation 17 leads to:

$$i = nFAC_o((P\delta^2 - P)/(\delta + P\delta^2 + P + P^2\delta))(D/\pi\tau)^{1/2}$$

$$\times \sum_{m=0}^{\infty} (-1)^m/(m + \beta)^{1/2} \qquad (20)$$

It must be emphasized that there is no rigorous derivation for Equation 20.

DC Currents in Square-Wave Polarography

In square-wave polarography, the capacitance and Faradaic currents resulting from the application of potential pulses (Equations 4 and 17-20) are added together with the DC currents. Christie and Osteryoung[8]

Table 1. Theoretical Effect of Pulse Size.

n	ΔE	one-half Peak Width Equation 18	one-half Peak Width Equation 19	% Difference in Peak Height
1	10	89.4	89.7	0.3
1	30	89.4	92.5	2.9
2	1	44.7	44.7	0.1
2	10	44.7	45.4	1.3
2	20	44.7	47.4	5.1
2	30	44.7	50.8	11.4
2	40	44.7	55.6	19.9
2	50	44.7	61.4	30.5
3	10	29.8	30.8	2.9
3	30	29.8	38.9	25.0

n = number of electrons, ΔE = step size in millivolts,

peak width = millivolts

studied the importance of the DC currents in pulse polarography. They concluded that the DC-Faradaic current does not represent an appreciable problem in pulse polarography. The DC-Faradaic current does cause a slight asymmetry of the shape of the pulse-polarographic peak and consequently causes a slight shift in the peak potential. However, since both the DC-Faradaic current and the pulse-Faradaic current are directly proportional to concentration, these effects are concentration independent and do not limit the sensitivity or accuracy of pulse polarography. This conclusion should be as valid for square-wave polarography in general as for the special case of pulse polarography.

The situation regarding DC-capacitance current is considerably more complex than with the DC-Faradaic current. The DC-capacitance current is of special significance since it is independent of concentration and acts to limit the sensitivity of square-wave polarography. There are actually two factors in the DC-capacitance current. The first factor is evident from an examination of Equations 3 and 17. The DC-capacitance current is proportional to the rate of growth of the electrode surface and therefore inversely proportional to the cube root of the time in the drop life. The pulse-Faradaic current is proportional to the area of the electrode surface and therefore proportional to the 2/3 power of the time, t, in the drop life. Thus the ratio of the pulse-Faradaic current to the DC-capacitance current is directly proportional to the time, t. This DC-capacitance current should be nonexistent with a fixed area electrode such as a hanging mercury-drop electrode or a rotating disk electrode.

The second factor in the DC-capacitance current results from the fact that this current is a function of electrode potential. Thus the DC-capacitance current before the pulse application will be different from that after pulse application. Figure 2 depicts the capacitance current when a pulse is applied during a drop. Curve 1 indicates the DC-capacitance current if the pulse were not applied, while curve 2 indicates the DC-capacitance current if the electrode drop had grown at the potential of the pulse.

In the pulse polarograph of Barker and Gardner[10], the current was measured only after the pulse application (point b in Figure 2). Parry and Osteryoung[6] introduced the use of a differential measurement in which the current before the pulse application is subtracted from the current after the pulse application (b - a in Figure 2). The first factor in the DC-capacitance current discussed above is equivalent to the difference, b' - a, in Figure 2. The second factor is the difference, b - b', in Figure 2. Christie and Osteryoung[8] pointed out the importance of the total difference, b - a, while Sturrock and Carter[9] pointed out that the difference, b' - a, is small compared to the difference, b - b'. The second factor, like the first, should vanish for a fixed area electrode, leaving the pulse-capacitance current and/or the electronic noise, as the primary factor limiting sensitivity.

Sampling Times

The theoretical equations discussed above do not establish optimum values of the experimental parameters of τ, ΔE, and the times(s) at which current is sampled. Hereafter the time between pulse

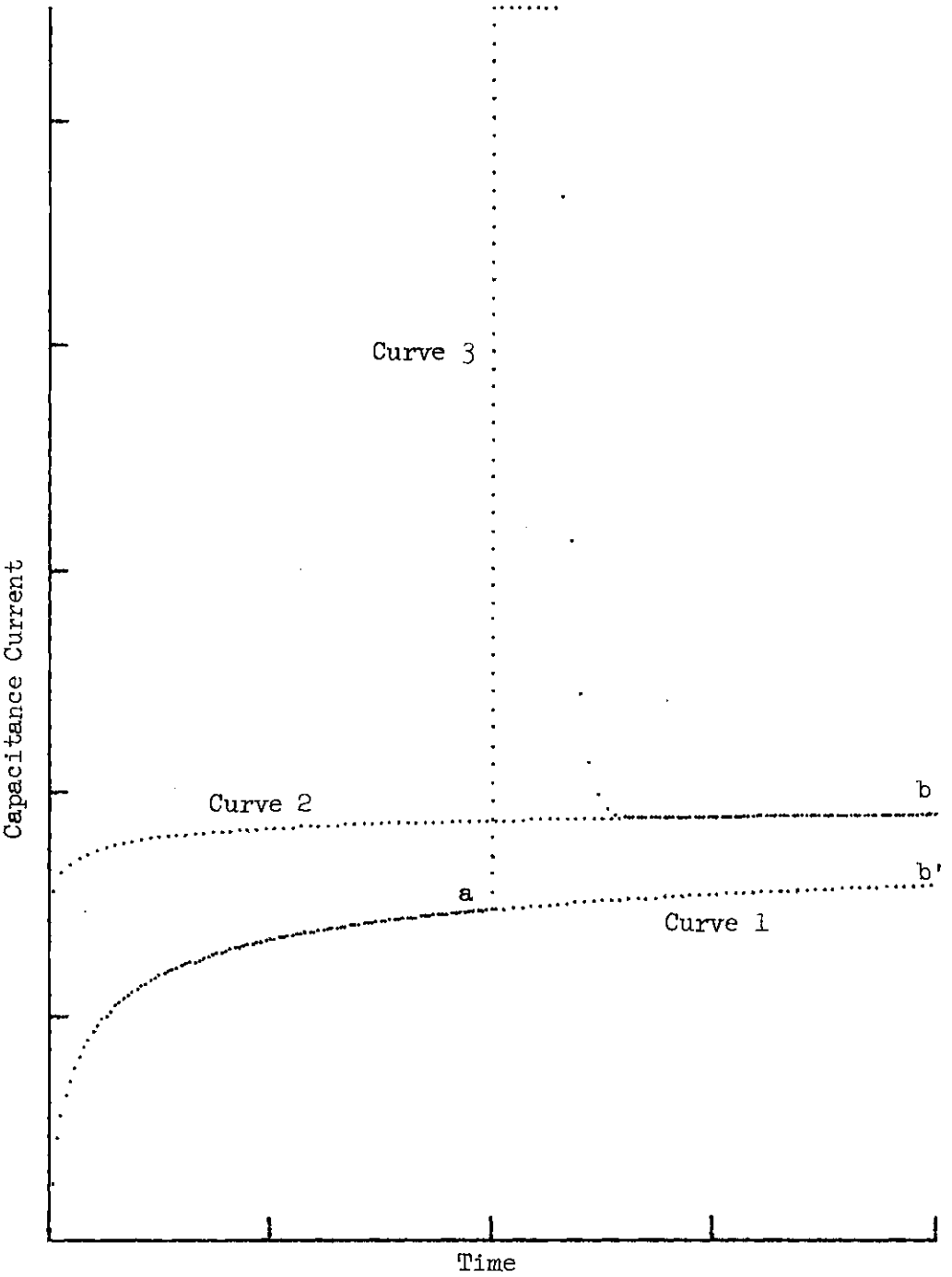

Figure 2. Pulse and DC Capacitance Currents Versus Time.
Curve 1, DC Capacitance Current at Potential Before Pulse.
Curve 2, DC Capacitance Current at Potential After Pulse.
Curve 3, Sum of Pulse and DC Capacitance Currents.

application, or relaxation, is called the delay time. Barker and Jenkins[4] used a square-wave frequency of 225 Hz, sampled the current late in each half cycle, and plotted the difference between the two halves versus the DC-sweep potential. The difference current was heavily filtered before recording so that some averaging over multiple square impulses was obtained. Apparently believing that the remaining capacitance current observed in square-wave polarograms was due to incomplete rejection of pulse-capacitance current, Barker experimented with lower square-wave frequencies in order to increase the delay time. Finally, Barker and Gardner[10] extended this idea to the limit and applied only one pulse per drop and thus introduced pulse polarography. In the commercial instruments (Southern-Harwell Models A1300 and A1700) based on Barker's design, the time delay is variable from 2 to 40 milliseconds. Later instruments have used delay times of 40 milliseconds or greater.

While it is clear that the ratio of pulse-Faradaic current to pulse-capacitance current will continue to increase as the delay is increased, it is necessary to consider other factors in determining the optimum delay time. As the delay time is increased, the absolute value of the pulse-Faradaic current decreases exponentially as $t^{-1/2}$. Thus the pulse-Faradaic current at 400 microseconds will be ten times larger than the value at 40 milliseconds. Once the pulse-capacitance current has decayed to a sufficiently small fraction of the pulse-Faradaic current, further delay before sampling should only result in loss of signal and a poorer signal to noise ratio. While Sturrock and Carter[9] suggested that an optimum time delay should exist

and reported some theoretical calculations, no experimental study of these factors has been reported. One of the goals of this study is an experimental evaluation of the optimum time delay before sampling and the effects of concentration and positive feedback (see below) on the value of this optimum time delay.

Positive Feedback

Modern polarographs operate with a three-electrode cell in which the reference electrode is used to measure the potential of the test electrode (usually a DME) without drawing appreciable current from the cell. This configuration results in only a small error in the measured potential because most of the cell resistance is compensated by the circuit. This resistance compensation, inherent in the three-electrode control circuitry (potentiostat), also markedly reduces the effective rc product of the cell that determines the decay rate of the pulse-capacitance current (Equation 4). The end result is that the pulse-capacitance current becomes negligible in comparison to the pulse-Faradaic current at a much shorter time after pulse application than with a two-electrode cell configuration such as used by Barker[4,5,10].

If a portion of the cell current is converted to an analogous voltage and this signal applied to the input of the potentiostat, the applied voltage is increased causing a more rapid change in electrode potential. The result of this positive-feedback technique is that the effective cell resistance is decreased even more than by the three-electrode configuration alone and the decay time for the pulse-capacitance current is decreased further. The theory and circuits for

the positive-feedback technique have been reported by several workers, notably Brown[11].

Liddle[3] reported the application of positive-feedback to square-wave polarography. However, no work has been reported that quantitatively relates the effects of positive-feedback on the rejection of pulse-capacitance current and the shape of the background curve (residual current) in square-wave polarography. Such a study is one of the goals of the present work.

Noise Rejection and Signal Averaging

Electronic instruments in general are plagued by electronic "noise" and polarographs are no exceptions. The usual response to this problem has been to use filter circuits. Often these filters are passive resistance-capacitance networks. However, more recently, active filters and other noise abatement techniques have become more common.

Resistance-capacitance filters, of sufficiently long time constants to effectively filter the noise, usually result in a heavily damped output signal that leads to a tailing or distortion of the peak in a recorded polarogram. In addition, effective use of such filters requires a repetitive signal with a repetition rate significantly higher than the cutoff frequency of the filter. In square-wave polarography, the frequency of the square-wave signal can be fast enough to make filtering effective. However, in pulse polarography, the repetition rate is equal to the drop time (typically 4 seconds) and it is not feasible to filter after the current measuring stage in the instrument. Thus, most of the noise filtering must be performed

during the current-sampling period in pulse-polarography.

Commercial pulse polarographs often use a period of 16.7 milliseconds during which the current signal is sampled by a circuit with a long time-constant network. This sampling window is used because it is the time period for one cycle of the 60 Hz power line that supplies power to the instrument and also is the most apparent source of electrical noise. However, until recently[12], no attempt was made to synchronize the operations so that the two current samples for the difference measurements were initiated at the same point in the 60 Hz cycle.

Sturrock and Carter[9] advocated the use of a gated analog integrator as the current sampling device, thereby filtering high frequency random noise and obtaining a larger signal than obtained by conventional filter circuits. In addition, since their instrument was a square-wave polarograph rather than a pulse polarograph, it was feasible to apply filtering after the current sampling stages of the instrument.

Summary

From the discussions in this chapter, it is obvious that there are many variations possible within square-wave polarography. However, most instruments are designed with a fixed delay time, a fixed sampling window, and either a continuous square wave or else only one pulse per drop. These fixed factors, selected during the design of the instrument, frequently seem to be badly chosen in view of the theoretical discussions above. The major purpose of this work is to experimentally and quantitatively evaluate the importance of variables such as

positive-feedback, number of square-waves per drop, time delay, length of sampling window, time in drop life, signal averaging, and other noise reduction techniques.

Such a study requires an instrument with great flexibility in the timing of potential changes and current measurements. It also requires numerical analysis of the noise levels and magnitude of base lines versus the peaks in the polarograms. The ability to obtain a series of polarograms, for comparison, in a short period of time is also mandatory. These requirements dictate the use of an instrument in which the timing and data analysis functions are handled by a digital computer. Details of the instrumentation are discussed in Chapter II.

CHAPTER II

INSTRUMENTATION, EQUIPMENT AND REAGENTS

Introduction

A polarograph is an instrument that can apply a voltage signal to an electrode in an electrochemical cell and measure the current passing through the cell. Early instruments operated with a two-electrode cell. One electrode is small in area so that concentration polarization can be developed readily. This electrode is usually called the test electrode or working electrode and in most cases is a dropping mercury electrode. The other electrode is a reference electrode, usually a saturated calomel electrode. The reference electrode in a two-electrode cell must be of relatively large surface area to minimize the development of concentration polarization at this electrode.

A serious problem with a two-electrode cell is that a portion of the voltage applied to the cell is expended to overcome the ohmic resistance of the cell. Thus the effective potential of the test electrode is not equal to the applied cell voltage minus the potential of the reference electrode. This error (usually called IR error) varies as the cell current varies. Modern polarographs use a three-electrode cell to minimize this IR error.

In a three-electrode cell, the third electrode is called the counter electrode or auxillary electrode. The cell current is passed

between the test electrode and the counter electrode while the reference electrode is used to measure the potential of the test electrode. No appreciable current is drawn from the reference electrode thus minimizing the amount of IR error in the measured potential and allowing the use of a small area reference electrode.

The portion of the polarograph that is connected to the electrochemical cell, and serves to control the potential of the test electrode with reference to the reference electrode, is called a potentiostat. The complete polarograph also includes sections to generate the voltage signals to be applied to the potentiostat, and sections that measure and process the cell current for the readout device. For pulse and square-wave polarography, discussed in Chapter I, timing circuits are also necessary to control the drop detachment, application of potential pulses, and current measurements.

In order to test various aspects of the theory for square-wave polarography, it is necessary to have considerable flexibility in timing, control, and readout circuits. An instrument, built and described by J. Liddle[3], was available for this study but did not have the necessary flexibility in the timing and current measuring circuits. Previous experience indicated that the only way to obtain the necessary flexibility, and also to reduce the time needed for data work up, was to replace the existing timing and control circuits with a small digital computer. The remainder of this chapter discusses various features of the hardware portions of the instrument while Chapter III discusses the programming (software) needed to make the computer carry out the experiments.

The overall organization of the instrument can be seen from Figure 3. The arrow heads indicate the direction of the information flow. The dashed line in Figure 3 encloses those components mounted in the polarograph cabinets. The cell is mounted inside a separate, grounded, metal cabinet which serves as an electrostatic shield.

Potentiostat and Cell Current to Voltage Converter

The potentiostat and current to voltage converter were previously described by J. Liddle[3]. Only minor modifications in these circuits were needed for this study. The sample and hold circuits that Liddle used between the two stages of current amplification were bypassed. Shielded cables were used to connect the potential (E in Figure 3) and current (I in Figure 3) signals to the differential inputs of the multiplexer on the computer.

In order to simplify the computer interface, it was decided to retain the manual controls for current gain and positive-feedback. All voltage signals were input to the potentiostat through the digital-to-analog converter.

Digital-to-Analog Converter

The digital-to-analog converter (DAC) is the device that converts a binary signal from the computer into an analog voltage signal suitable for input to the polarograph. In the early stages of this work a 10-bit DAC, manufactured by Analog Devices, was used. The 10 binary bits used to control the unit represent up to 1024 levels so that a resolution of 1 part in 1024 was possible with this unit. A voltage divider was used to drop the ± 10 v output range of this DAC to

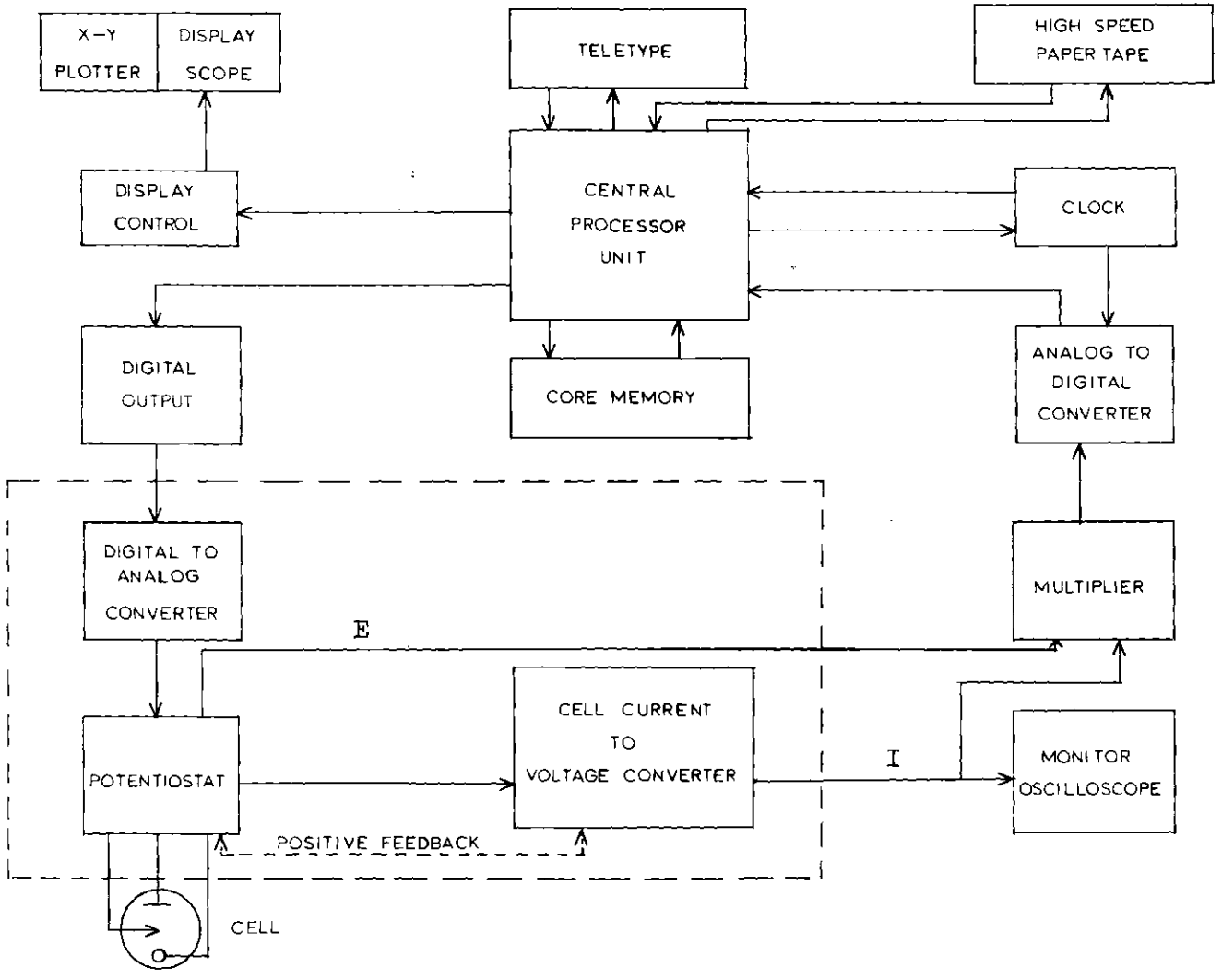

Figure 3. Block Diagram of Instrument.

±1.7 v. Each step of the DAC was equivalent to 3.3mv. However, it was soon realized that a DAC with greater resolution was needed for some of the experiments and consequently this unit was replaced.

The greatest resolution possible with one 12-bit computer word is 1 part in 4096. Thus a 12-bit DAC, with output divided down to ±2 volts, would have a step size of 0.98 mv which was adequate for this study. However, another factor to consider is the precision.

Usually a DAC has a guaranteed precision of $\pm\frac{1}{2}$ of the least significant bit (LSB). The LSB has a value equal to the smallest step, in this case 0.98 mv. Thus if a 12-bit DAC were used in this application, the step size would be 0.98 mv and the precision would be ±0.49 mv.

The DAC selected was a 16-bit DAC manufactured by Datel Systems. While only 12 bits could be controlled by the computer, the particular 12 bits selected to be controlled were the 12 most significant bits (MSB) rather than the 12 LSB. This still resulted in 4096 steps, but the precision was $\pm\frac{1}{2}$ LSB. The result was a step size of 0.98 mv with a precision of ±0.03 mv rather than the ±0.49 mv which would have resulted had a 12-bit DAC been employed.

The DAC was mounted within the polarograph cabinet to minimize noise pickup between the output of the DAC and the input of the polarograph. The 12-bit, parallel, digital signals to the DAC were transmitted from the digital output of the computer via a ribbon cable.

Digital Output

Upon command from the central processor of the computer, the

digital output device transmits a 12-bit binary word (parallel format) to an external device, in this case, the DAC. The digital output device also serves as a buffer so that the external device cannot interfere with the operation of the computer. The bufffered digital output (DR8-EA) manufactured by the Digital Equipment Corporation is used for this purpose. However, the unit was modified for this study for the following reason.

As the DR8-EA was originally designed, the computer command, DBSO, caused any output bit of the DR8-EA to be set to the "one" state if the corresponding data line from the computer was in the "one" state. If the corresponding data line was in the "zero" state, the output bit remained unchanged from the previous value regardless of whether the previous value was a "one" or a "zero". To clear a bit (i.e. set it to the zero state), it was necessary to issue a different computer command, DBCO, and to have a "one" in the corresponding data line.

Thus to change from one 12-bit value to another, it was necessary to first clear all bits with a DBCO command and then to get the desired bits with a DBSO command. This resulted in a period of 2.4 microseconds between the old value and the new value during which the output was "zero" in all 12 bits. This all "zero" configuration caused the output of the DAC to go to its maximum voltage for 2.4 microseconds. The result of all this was simply that the DAC output, and hence the electrode potential, went to +2 volts between each potential setting. This was clearly intolerable.

The DR8-EA was modified to change from any value to any other value on a single DBSO command without first having to clear with a

DBCO command. In the modified version the DBSO command causes each bit to be set to the state of the corresponding data line ("one" or "zero").

Computer

The several tasks of the computer are: to generate all of the necessary control signals for the polarograph at the desired times, to sample the cell current at the desired times, to process the current signals and display them on the display oscilloscope during the running of the polarogram, to prepare permanent (hard) copies of the polarograms on the X-Y plotter, to perform statistical analysis on base lines, and calculate the output parameters (see Chapters III and IV). Flexibility is obtained because at the start of each polarogram the operator enters, via the teletype, the various parameters to be used.

The computer used in this study was a Lab PDP-8e manufactured by the Digital Equipment Corporation. It consists of the central processor unit (CPU), 8192 words of 12-bit core memory, a 10-bit analog-to-digital converter (AD8-EA), an 8-channel analog preamplifier and multiplexer (AM8-EA), a point plot display control (VC8-EA), a real-time programmable clock (DK8-EP), a display oscilloscope (VR-14), a high-speed paper tape reader and punch (PC8-E), and a teletype.

The multiplexer acts as a switching device so that more than one analog signal can be sampled and converted to digital representation by the analog-to-digital converter (ADC). In this study only two channels of the multiplexer were used. One channel sampled the cell current and the second sampled the electrode potential.

Clock

All timing functions were performed by the digital clock of the computer. The clock can be started by a command from the computer or by an external event triggering one of the Schmidt Trigger inputs of the clock. At the end of the prescribed period of time, the clock signals the computer via the interrupt service line. The computer then takes the required action such as changing the electrode potential via the DAC, or sampling the cell current via the ADC, etc. In some cases the clock directly signals the ADC to make the conversion from analog to digital and to have that information waiting for transfer to the central processor.

The rate at which the clock counts can be varied, on computer command, from 10^{-6} seconds to 10^{-2} seconds in powers of ten. The number of clock counts, or ticks, before the clock generates an interrupt signal for the computer, can be varied from 1 to 4096. Thus combinations of clock rate and number of ticks give great flexibility in timing.

In this study, it was decided to synchronize operations with the 60 Hz power line signal so as to minimize noise pickup from this source. To accomplish this, one of the Schmidt Trigger inputs of the clock is tied to the 60 Hz line and signals at this input are used to start all timing sequences.

Relay

The computer is equipped with a special interface for controlling laboratory operations. The only use made of this interface in this study is the use of a reed relay to operate the detaching

of the drop in the cell. Upon computer command the relay closes, actuating a solenoid which strikes the capillary of the DME causing the electrode drop to fall off the tip of the capillary. This is the initial action of the experimental sequence for each new drop.

Associated Equipment

Cell

The cell in all cases was a 100 ml Berzelius beaker with a rubber stopper pierced to accept the various electrodes.

A medium porosity gas dispersion tube was employed for deaeration of the solution with nitrogen. After deaeration was completed, the tube was raised above the solution and used to maintain a blanket of nitrogen gas over the solution.

Electrodes

In all experiments a three-electrode cell, consisting of a counter electrode, a working electrode, and a reference electrode was used.

DME. A Sargent-Welch 2-5 sec capillary was used in all cases, connected by a short piece of tygon tubing to a piece of 7mm glass tubing which was affixed to a meter stick. This glass tubing was connected by tygon tubing to the reservoir containing the mercury. By using the meter stick to measure the height of the mercury column, a fairly high degree of precision was obtained in the drop growth rate.

Counter Electrode. This consisted of a flat piece of platinum ribbon sealed in a glass tube. This ribbon was welded to a wire and then sealed inside the tube.

Reference Electrode. In all cases a porous-ceramic junction Fisher calomel electrode was used.

Oscilloscope

In all cases a Tektronix Model 564B Storage Scope with dual-trace Type 3A6 plug-in was used. The time base was a Type 3B4.

Recorder

A Hewlett-Packard Model 7040a X-Y recorder was used to make permanent copies of the polarograms being displayed on the display oscilloscope. The pen of the recorder could be lifted and dropped under computer control so as to make point plots.

pH Meter

All pH readings were made with a Corning Model 7 pH meter after calibration with 0.05 F potassium acid phthalate.

Reagents

All chemicals used in this study were either "Baker Analyzed" or Fisher reagent grade, except for the mercury which was triply distilled by Bethlehem Apparatus Company.

In the initial stages of this study, the water used to prepare solutions was taken from a Barnstead still and then passed through a Crystalab Deeminizer. The resulting water had a salt concentration of less than 0.2 ppm, as NaCl, as indicated by conductivity measurements. During the course of the study, a water purification system was constructed which consists of two mixed-bed deionizer cartridges in series followed by a particulate filter. This system produces water of less than 0.01 micromhos/cm which exceeds the ASTM standard for "Reagent Water".

CHAPTER III

SOFTWARE

Introduction

One objective of this study was to develop general purpose software for the control and acquisition of electrochemical data using the hardware system described in Chapter II. This required the software to meet four conditions: (1) the software must provide all timing control for the application of potential changes and acquisition of data, (2) the software had to do preliminary processing of the raw data in the time between individual acquisitions, (3) the software had to be controllable via a teletype input and be able to provide output to a variety of devices, and (4) the software must be capable of being easily modified as both hardware and experimental considerations changed. Due to the relatively high rate of data acquisition which would be used in the course of these experiments, use of a high-level and high-overhead language such as BASIC or FORTRAN would not be feasible. For this reason use of assembly language software was necessary.

A foreground-background software system was indicated because of the need to have both a high data rate and concurrent visual display. In this situation the foreground program does such tasks as timing, potential changes, data acquisition, and the initial reduction of raw data into a form suitable for permanent high-density storage.

The background program handles all tasks which require input and output (i.e. teletype, hard plotter, display scope, and any further reduction and processing of the permanent data that are stored by the foreground program). These two programs are interconnected by the interrupt routines. In order to facilitate program changes at a later date, the foreground and background programs were written as small sections of linear program and attached to each were subprograms (Each subprogram would have a specific function, and if a function needed to be changed, only the appropriate subprogram would be changed). This allowed for future modifications with the least amount of change in the program. The use of these subprograms, and their use of subroutines, unfortunately resulted in a slightly longer program and therefore a decreased acquisition rate.

The software system that was written not only met the needs of this study, but should be general enough to be usable for future studies. The manner in which the program was written allows the experimenter to test a wide variety of hypotheses with regard to the timing and size of potential change, the rate of data acquisition, the total time to generate a particular run, and time averaging (by varying the number of points taken).

The software system used for program development was the standard DEC[13] paper tape system. There were three utility programs used in this system for the development of machine language software. EDITOR was the first of these programs. In EDITOR the programmer enters the program in the form of a specified set of mnemonic codes, each code consisting of alphanumeric characters in a specified order,

rather than binary code. In using the EDITOR program the programmer need not worry about the real address of a referenced line or code. Instead, he references any other location by symbolic addressing. If a particular location in a developing program is to be referenced by another part of the program, this location is given a symbolic name, and it is this name that is used when referencing that location.

PAL III was the second utility program used. This program is a three-pass assembler. During the first pass, PAL III reads the symbolic paper tape generated by EDITOR and compiles a set of absolute addresses for each symbolic reference used. It is during this pass that PAL-III also generates Teletype (TTY) messages indicating any symbolic or syntax errors. The second pass generates a binary paper tape using both the symbol table generated in pass one and the symbolic tape from EDITOR. In the third pass the assembler prints a complete listing of the program in both mnemonic code and the equivalent octal code. In order to facilitate this work the standard PAL III tape was modified such that certain special codes, used by interfaces particular to this hardware, would be recognized.

The third utility program used was CROSSFIELD-ODT. This program is a combination and modification of two different programs. ODT is a standard debugging routine developed by the Digital Equipment Corporation, but it has the limitation of having to operate in the same core memory field as the program to be debugged. Since the software system that was developed required most of one field, ODT could not be used. The second program, CORE WINDOW, was obtained from DECUS[14] and has the same limitations as ODT. These two programs were

modified so that the combined program is placed in one core memory field and the program being developed in the other. This allows various programs to be changed via the TTY and the resulting changed programs to be punched out in binary format via the high-speed paper tape punch. This program found much use when minor changes had to be made and checked out, without going through the longer procedure of EDITOR and PAL III.

To provide a logical order, the discussion of the entire software system will be divided into four main areas: the interrupt handling routines, the foreground program, the background program, and the input-output subprograms (these subprograms are separated from the background program for discussion, but in reality they operated basically with the background program). Figure 4 shows the overall structure of the electrochemical software system.

Interrupt Handling Routines

The interrupt handling routine enables the foreground and background programs to work in conjunction. Both the foreground and background programs must be able to work alone without having direct interaction with each other. The interrupt handling routine is the link between the foreground and the background programs. This routine contains the necessary information as to which program is to be run next and the appropriate address needed for the next step. The interrupt provides a means for some external event to cause program control to be relinquished by the background program in favor of the foreground program. It is the task of the interrupt routine to store

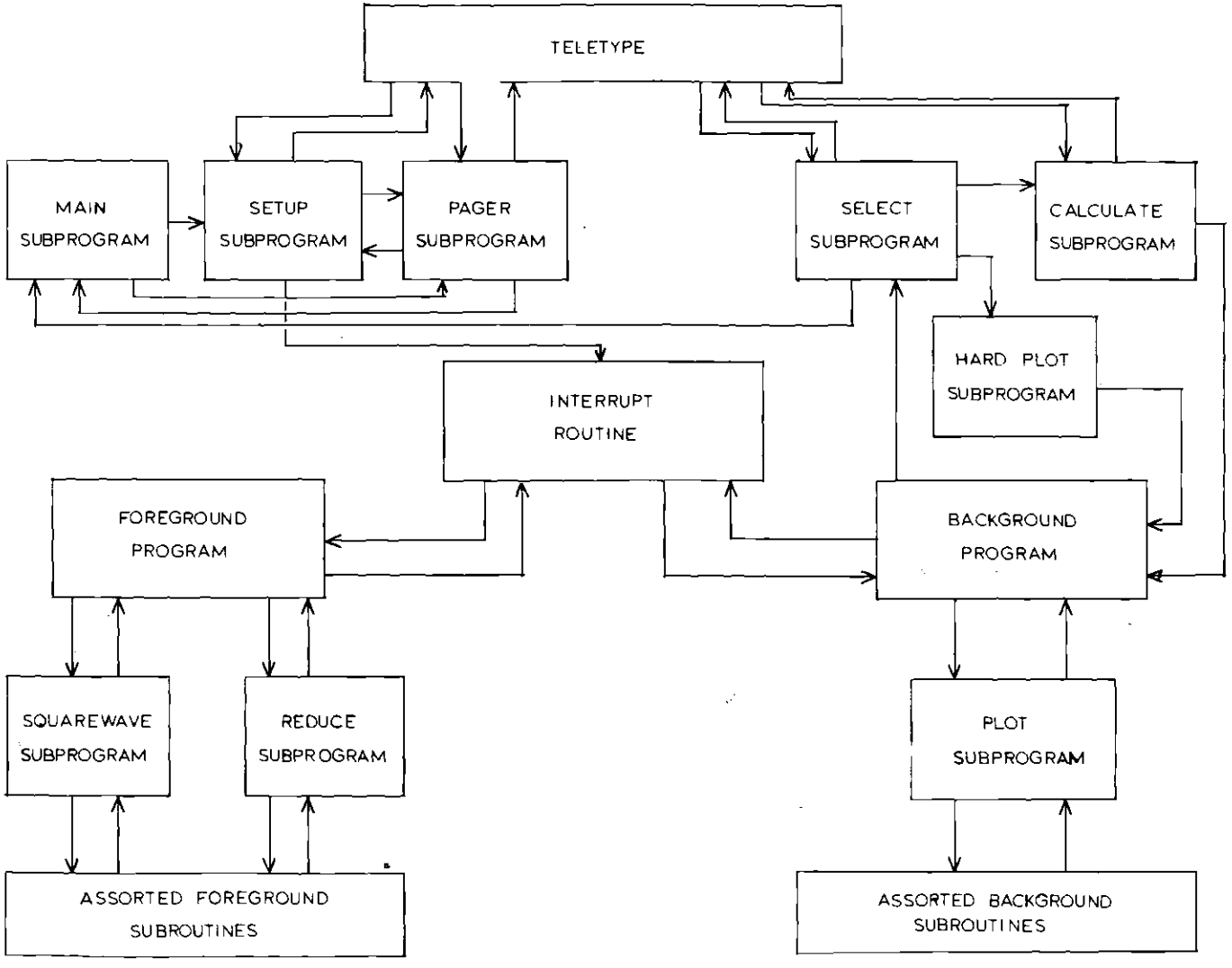

Figure 4. Block Diagram of Software.

any necessary return addresses and then transfer control to the foreground program.

In the particular case of the electrochemical software system, the only external device which can cause an interrupt is the clock. The background program has no control over when it can be interrupted. The foreground program informs the interrupt routines exactly where to go on relinquishing control on the next interrupt. At no time does the background program or the foreground program have the knowledge of where the other is, and it is this transparency which is the primary requisite for a successful foreground-background program system.

One of the problems faced by the programmer, when designing the interrupt routines, is maintaining transparency. A problem arises if both the foreground and the background programs make use of a common subroutine. The problem is that if a segment of the background program is using a particular subroutine and has not finished with it before the interrupt occurs, the starting address of that subroutine contains the return address to the main body of the background program. If, following an interrupt, the foreground program then calls the same subroutine, the starting address of the subroutine would contain, not the return address of the calling routine of the background program, but, instead, the return address to the main body of the foreground program. When the foreground program is done and returns control to the location where it was when the interrupt occurred, that subroutine continues to its end and jumps back to whatever location is in the starting address of the subroutine. In this case, the last address located there does not point into the background program, but rather

into the foreground program.

In most cases the routines are short enough that there is no problem to duplicate them for the foreground and background programs, thus maintaining transparency. However, a special problem arose with the floating-point package. There was insufficient core memory to duplicate the standard floating-point package, so it was necessary to write a new, limited version for use by the foreground program. This limited version of the floating-point package uses a two-word format rather than the standard three-word format. In both formats the leftmost bit of the first 12-bit word is designated as the sign bit. The remaining bits represent the magnitude of the exponent. In both formats the next word is the mantissa word, but in the three-word format a third word is used as a low-order mantissa word.

Background Programming

The primary background subprogram, PLOT, has the function of displaying the incoming data as it is acquired. The subprogram is initially entered by the return through the interrupt system. This program first divides the X-axis into equal sections, the number of which is determined by the number of drops in the polarogram. Then it determines the minimum and maximum Y values up to that particular time and uses this information to scale the Y-axis. This procedure makes the display auto-ranging and results in the display being maximized. The display is continually refreshed until the next clock interrupt. After all the data has been acquired, the PLOT subprogram turns the interrupt off. The computer remains in the background

program until a new data run is initiated.

Foreground Programming

The foreground program consists of two subprograms. The first of these is SQWAVE, a subprogram designed to produce the proper sequence for the potential change in order to produce pulse and square-wave type excitations and to handle the proper timing for the input of data. The second, REDUCE, was designed to reduce the raw data to the format which is to be stored. In addition to these subprograms there are a number of subroutines which are used by SQWAVE and REDUCE and which allow the experimenter to make changes in the types of potential excitation and in the handling of the resulting data without having to reprogram completely. As in the rest of the program the emphasis is placed on versatility for future change by requiring only minor changes in the backbone part of the program and some changes in the subroutines.

SQWAVE's function is to produce potential changes which correspond to pulse or square-wave type excitations and then to measure the resulting currents. In this subprogram three variations are available which differ only in regard to the time when the data is taken. In the first variation a negative pulse is applied first, and then after a time delay, the subprogram initiates data acquisition for the negative side. Following the completion of data acquisition, an equal positive pulse is applied and after the same time delay, the positive side data is acquired.

The second variation can be used only with a single pulse.

In this case, current is measured prior to pulse application and after pulse application, and the difference is recorded. In the third variation, only the negative or positive side current is measured and recorded.

The REDUCE subprogram is divided into two sections. The first section was designed to retrieve the raw data that are deposited into the temporary buffers by SQWAVE and to take each pair of data (one data point each from the negative pulse and the positive pulse), subtract them, and then add the difference produced to all the other differences which have been done over the course of the entire drop. It is during this process that the subprogram makes use of the two-word floating-point package mentioned above. The second section of REDUCE transfers the processed data to the permanent buffer located in field one, reinitiates the software registers in preparation for the next use, and returns control to the main foreground program.

Input-Output Subprograms

These subprograms are used just before the foreground program is activated and just after it has concluded. For the most part, the first group of subprograms is used to initiate the foreground program. The first group consists of two subprograms and seven subroutines.

The subprogram, MAIN, forms the initiation part of the software system and has numerous functions. It provides a means to reset or clear any peripheral flags so that these peripherals are ready to be used by the various programs. Another function is to ready the software registers used by the interrupt routine. The third function

is to provide calls to the subroutines, DATE and RUN. A final function of MAIN is to provide a means for the programmer to enter a heading on a particular run without this information being stored.

SETUP is a subprogram which allows the operator to input various parameters needed in the experiment. The subprogram consists of a series of routines in sequence. Fourteen of these routines deal with the entering of parametric information into the software system. Generally, these routines are made up of a call for the subroutine PAGER which is the general message handler, followed by either a call for the octal input subroutine, OCTIN, or the decimal input subroutine, FINP. Following these subroutines are the instructions for storing the information in the appropriate manner and in the appropriate locations. Although there are fourteen routines for input of data, many would not be needed in any particular experiment. Routines which are not needed can be deleted readily.

The final action of SETUP is to initiate a waiting loop in which the program waits until the operator has all external equipment ready. Upon activating Schmidt Trigger number one, the waiting loop is exited. The program then clears the clock and restarts it with the proper directives (i.e. rate and number of ticks before interrupt, etc.) from the program. Then this subprogram relinquishes control to the interrupt handling routine.

The second group of input-output subprograms include four subprograms and four main subroutines. In addition several subroutines are used which are also called by the background program PLOT. PAGER is designed to aid in the output of desired messages to the TTY.

Within this subprogram resides the text of all messages normally typed by the program.

SELECT acts as a pointer subprogram to either CALC or XYPLOT, both of which are associated subprograms. The function of SELECT is to match two letter identifiers from the TTY with the correct pointer to the start of the desired routine, and using that pointer, turn over control to the desired routine. An additional function is to identify when the operator wants to restart the software system for the next run.

XYPLOT is a subprogram to provide a means of transferring the polarogram shown on the oscilloscope to the X-Y plotter. The program is initiated when XY is typed on the TTY after all the data have been acquired.

The subprogram CALC functions as the interpreter for the experimental data which the foreground program acquires. The experimenter has to indicate via certain TTY inputs three sets of information: a left baseline, a right baseline, and the point which is the highest point in the peak. Using this information the program then automatically calculates and provides output via the TTY of the following information: average value of the indicated baseline, the value of the peak (P), the percentage of the average baseline with regard to the peak value (B%P), the peak value less the average baseline (P-B), the standard deviation of the baseline (rho), the value of the peak value divided by the standard deviation (P/rho), and the peak width.

CHAPTER IV

EXPERIMENTAL

Introduction

As discussed in Chapter I, one drawback in the design of standard instrumentation in the field of polarography is the relatively narrow range of variations possible with a given instrument. In Chapters II and III the basic instrument used in this work was discussed and the necessary programming was described. One result of the mating of a basic potentiostat and a digital computer is the ability to evaluate a number of different parameters fairly easily. The experiments investigated a variety of questions, from repeatibility of a set of measurements, and thus inherent error, to the determination of the best time delay between pulse application and current measurement. The significance of the work lies in the trends that a given experiment illustrates rather than in the values of the individual numbers. Thus preference is given to graphical presentation of the data although both tables and graphs are given in most cases.

Since a wide variety of experiments were performed, a general overview of this chapter is in order. The first item covered concerns standardization of experiments. In this section the design of the experiments is discussed. Next is a discussion of the various experiments related to the best time delay to be used in square-wave polarography. Following this, the effect of positive feedback on the time

delay is discussed. The next experiments deal with drop size variations and noise averaging. The last experiments deal with the effect of the baseline variability with the number of ADC levels used. The chapter ends with the conclusions based on all the experiments.

General Experimental Conditions

In order to allow for valid comparisons from experiment to experiment and even from run to run, it was decided to use a minimum of different solutions. To this end large quantities of solutions were made up initially and stored in polypropylene containers. The primary solution used in the course of the experimentation was:

Soln. A - 1.031×10^{-4} F Cd^{+2} with 0.1F KNO_3 and 1.0 ml conc. HNO_3 per liter

Most of the other solutions used were made up using Soln. A as the stock solution.

It was necessary to use standardized procedures during the course of experimentation. It was decided to run no more than eight polarograms, which would generally constitute one experiment, from a given aliquot of solution. By this means it was hoped that a minimum of solution aging would take place. If a particular experiment required greater than eight runs to complete, a change of solution was made following the eighth run and the ninth run was a repeat of one of the original eight. Using these rules it was felt that a minimum of outside interference would occur and runs within a given experiment could be successfully compared.

During the course of a particular set of runs, the potentiostat was always switched to the standby position following completion of a run, and the nitrogen bubbler was lowered into the solution. Again this standardized the external variables as much as possible.

The operation of the instrument as well as the long term integrity of the standard solution, was checked periodically by polarograph using the standard set of conditions. The standard set of conditions are given in Appendix I.

Determination of Range of Variability of Instrumental System

One of the first questions to be answered was how much variability was present just due to noise, voltage fluctuations, and general instrument variability. Without the above determination it would be impossible to determine if any trends seen in later experiments were real. To determine this variability it was decided to investigate the variability in B%P values in time. B%P is defined as the average baseline (found by averaging 20 points, 10 on each side of the peak) divided by the value of the intervening peak, multiplied by 100. The reason for the use of this particular value as compared to any other is that since the concentration of the species to be determined is proportional to the peak height minus the baseline height, this term is deemed the most significant.

Two separate experiments were performed. Each experiment consisted of four and five runs respectively spaced over a period of two hours. The two-hour time span was used since it was found that normally eight runs could be accomplished within this time span. During each

experiment, each run was completed using the same parameters (i.e. time delay, potential step, etc.). In addition each run was preceded by the same length of time of deaeration, mercury flow, and instrument standby. In this way these series were run in as identical a way as possible to the subsequent experiments. The solution used was the standard solution discussed earlier. The results of these two experiments are given in Table 2.

Table 2. Instrument Variability.

Series 1	1	2	3	4	5
B%P	0.74	0.75	0.84	0.88	----
Series 2					
B%P	0.83	0.83	0.81	0.77	0.84

	Variance	Mean	Range	Standard Deviation
Series 1	0.0035	0.80	0.14	0.068
Series 2	0.00062	0.82	0.07	0.028
Total of Both Series	0.002	0.81	0.14	0.0469

As will be seen later, these values demonstrated that most of the data collected indicate real trends rather than just data variance.

Delay Time

As has been discussed previously the prime motivation for this work was to determine some optimum parameters to be used in polarography to balance time of determination, sensitivity, and accuracy. Much

dissension has existed in this field over the optimum time delay following an application of a potential step. Delay Time values ranging from less than one millisecond all the way to 40 milliseconds have been reported. For this reason the delay time study was determined to be crucial. The study consisted of four experiments. The first experiment dealt with the standard cadmium solution (Solution A) and investigated the time span from 0.1 msec to 9.0 msec in eight runs. The second experiment refined the value of the optimum time found in the first experiment (approximately 1-2 msec). The third and fourth experiments investigated solutions where the concentration of the electroactive species was lower than that in the original solution. In these experiments, the time window during which current was measured was kept constant at 1.0 msec.

The first experiment in this study treated the delay time span of 0.1 msec to 9.0 msec. The results of this set of runs can be seen in Figure 5 and Table 3. From Figure 5 it can be seen that the B%P is quite high at times closely following the potential step. As the delay time was increased, the value of B%P rapidly decreased and seemed to reach a minimum between 1 and 2 milliseconds. The decrease in the B%P at short delay times was explained by the presence of pulse-capacitance current. During very short times, and at potentials where no reduction could be occurring (i.e. during the baseline), the pulse-capacitance current is the only major current available to increase the baseline. A further look at Figure 5 reveals that following the 1 - 2 msec. time span the B%P values again increase, though only slowly. During this time the pulse-capacitance current has been eliminated and

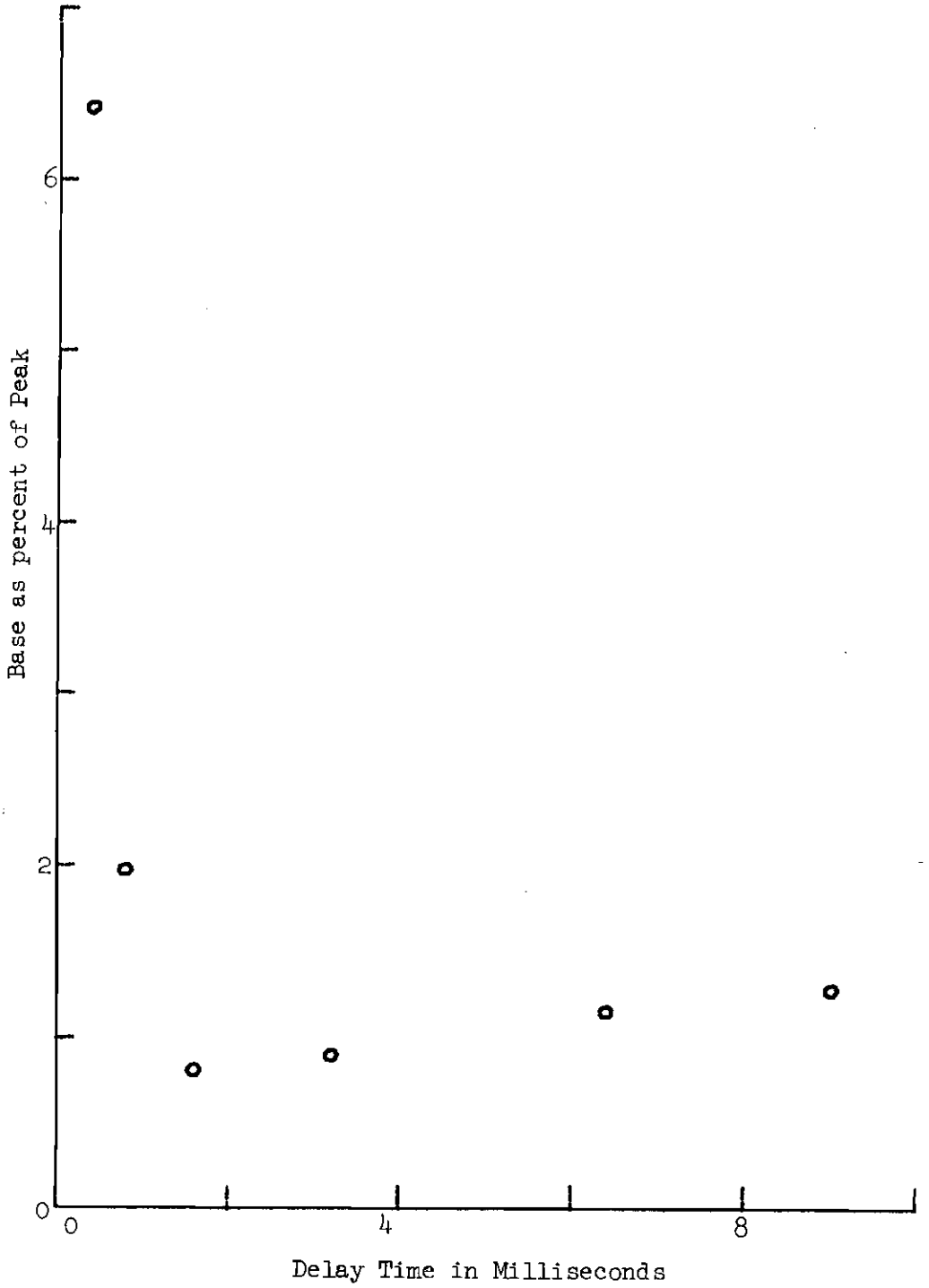

Figure 5. Base Percent Peak versus Delay Time for 10^{-4} F Cd in 0.1 F KNO_3. Large Time Scale.

Table 3. Current Decay (Large Time Scale)

Delay Time	B%P	P(arbitrary units)
0.1 msec	21.45	792,277
0.2 msec	19.78	802,552
0.4 msec	6.42	855,182
0.8 msec	1.97	730,744
1.6 msec	0.81	574,856
3.2 msec	0.90	430,744
6.4 msec	1.15	316,556
9.0 msec	1.28	265,350

the increase in the baseline with respect to the peak is due to the continued loss of Faradaic current with time while the baseline noise remains constant. This loss of peak height is shown in Table 3. If it is assumed that B%P increases linearly through the last four points, then at 40 msec one would expect the value of B%P to be 3.33. This indicates that the signal-to-noise ratio would be 4.11 times greater at 1.6 msec than at 40 msec which is the time usually used by commercial instruments. If the baselines were due only to pulse-capacitive current, theory would predict a fivefold signal-to-noise reduction by waiting 40 msec instead of 1.6 msec.

The second experiment in this study was an attempt to define better the minimum that the first experiment indicated. In this series of runs the same standard solution was used as in the first series, but the time delay span was only from 0.8 msec to 3.0 msec. This experiment was one of the few experiments containing more than eight runs,

and a change of solution was made after the eighth polarogram. As was stated earlier, whenever two solutions were used during a particular experiment at least one run was repeated in each series, and during this experiment the 1.0 msec delay time polarogram was duplicated. The two runs at 1.0 msec only differed by 0.03 B%P which shows the reproducibility from solution to solution. A further indication of the reproducibility comes from a comparison of the value for B%P at the time delay of 1.6 msec for the first and second experiments. In the first experiment at 1.6 msec the B%P was found to be 0.81, while in the second experiment it was found to be 0.84. Based on this there is strong evidence for the reliability of comparisons from experiment to experiment.

The data from the second experiment, shown in Figure 6 and Table 4, indicate that the true minimum in B%P occurred around 1.0 to 1.1 msec for the solution in question. Even when the statistical data from Table 2 is taken into account, a minimum is still indicated in the region of 1 to 2 msec, a time well short of that advocated in much of the current literature.

The final two experiments in this study investigated the time delay at lower concentrations of the electroactive material. In these experiments the electroactive species was 1×10^{-5} F, but the supporting electrolyte was held at the same level as previously used. As in the two experiments at the higher concentration the first experiment was run to determine the general shape of the time delay versus B%P curve (see Figure 7), while the second experiment was run to get a refined value for the location of the minimum (Figure 8). The

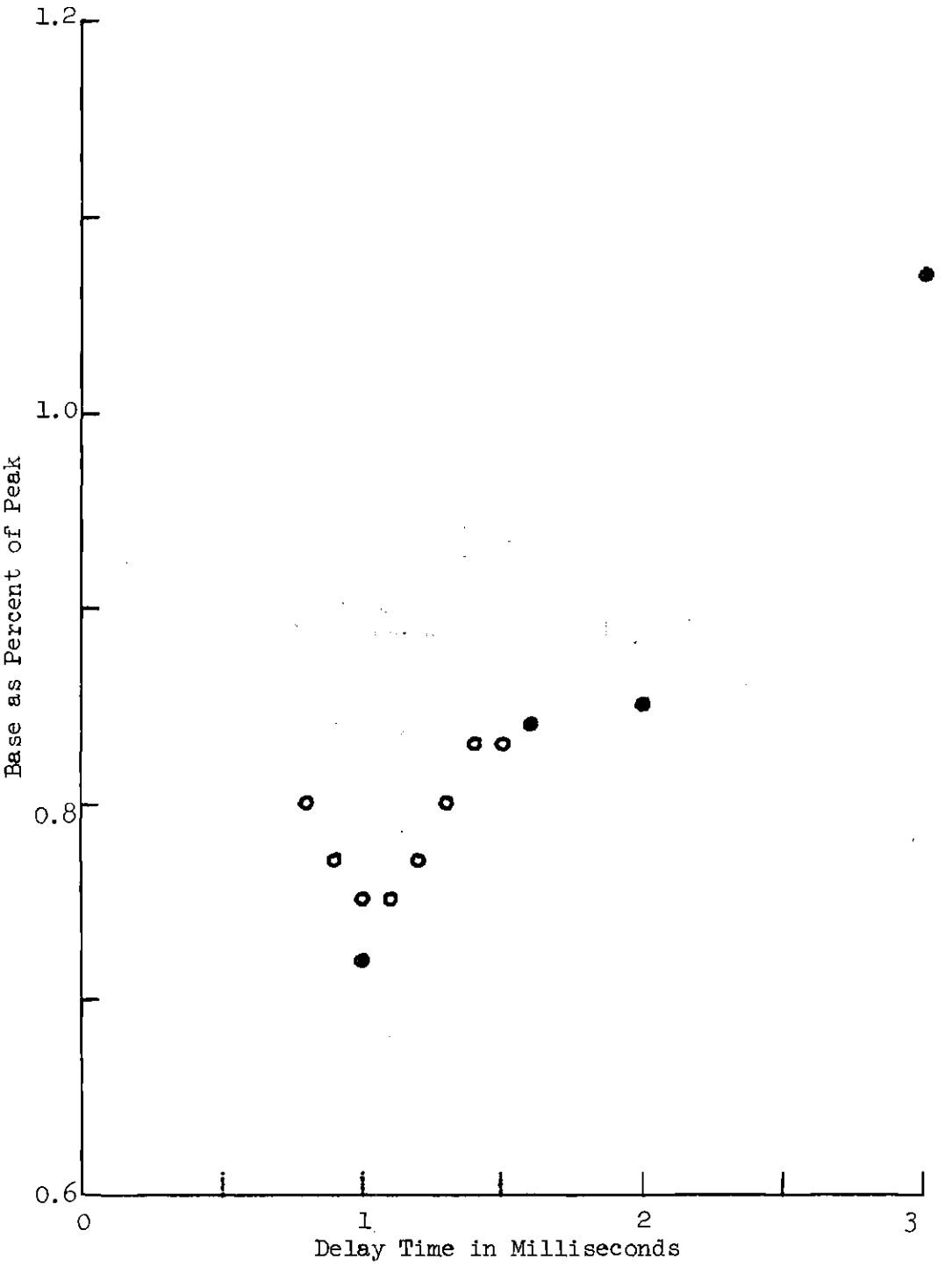

Figure 6. Base Percent Peak versus Delay Time for 10^{-4} F Cd in 0.1 F KNO_3. Small Time Scale. • indicates Second Run.

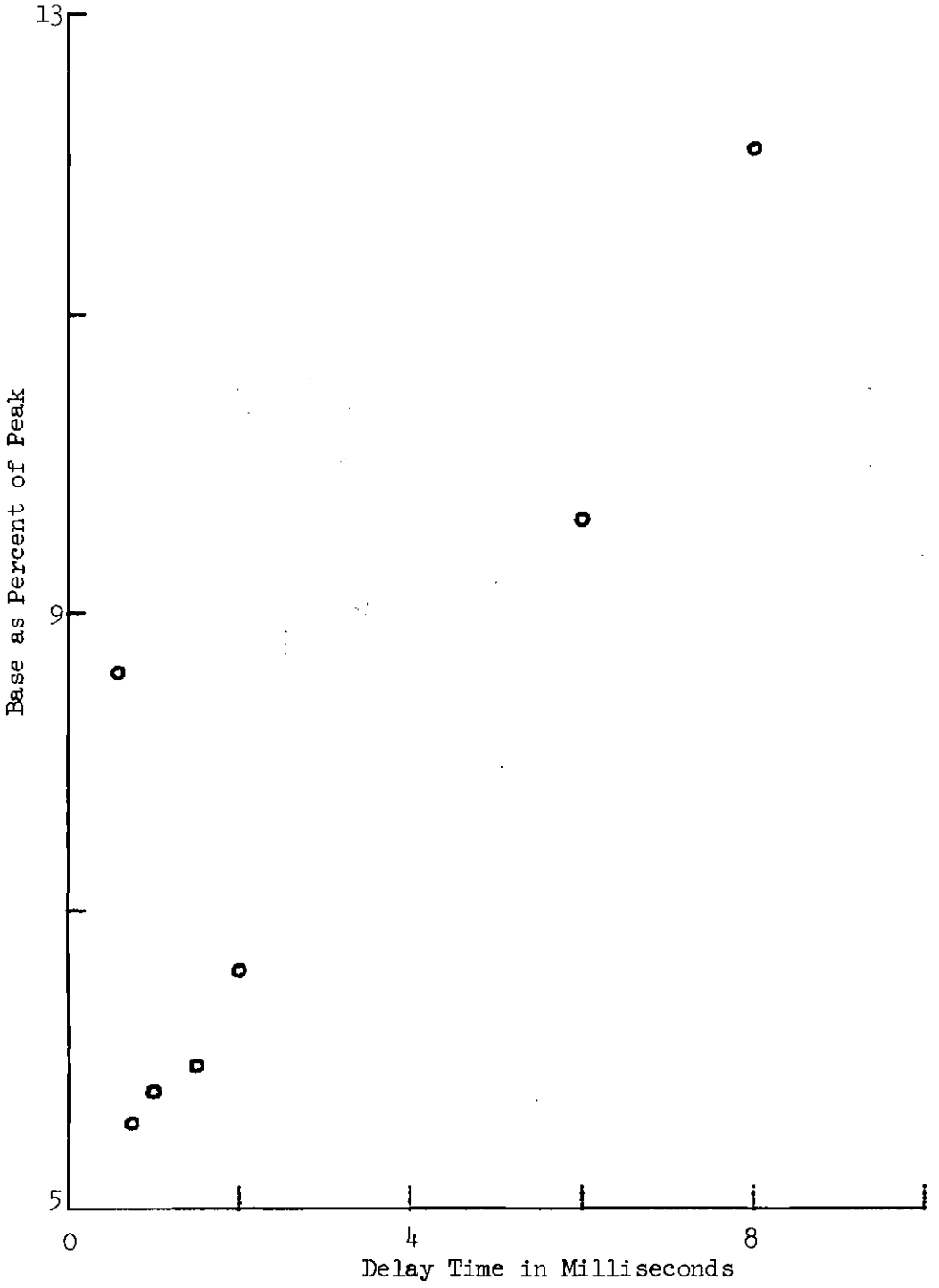

Figure 7. Base Percent Peak versus Delay Time for 10^{-5} F Cd in 0.1 F KNO_3. Large Time Scale.

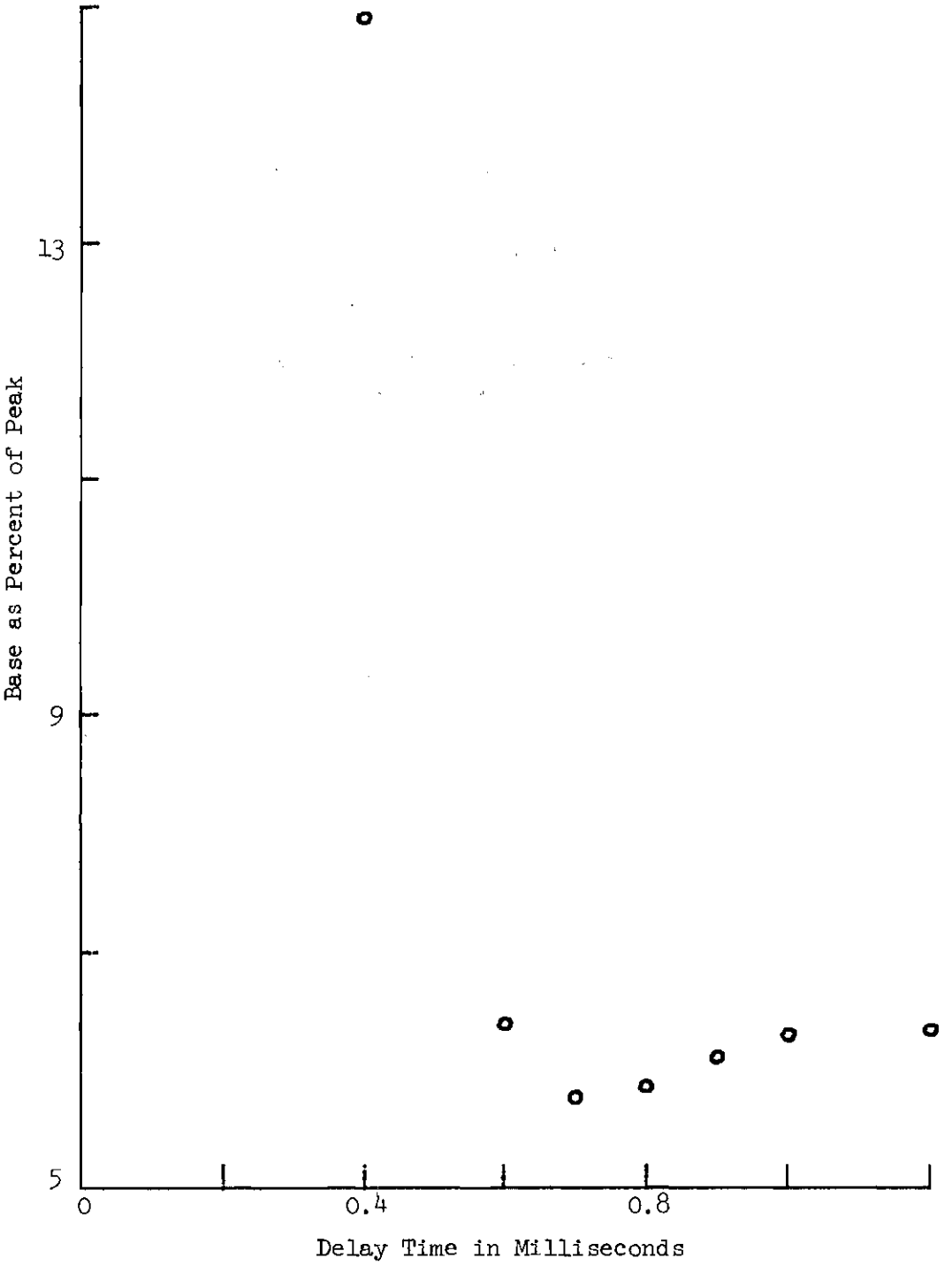

Figure 8. Base Percent Peak versus Delay Time for 10^{-5} F Cd in 0.1 F KNO_3. Small Time Scale.

Table 4. Current Decay (Short Time Scale)

Delay Time	B%P
0.8 msec	0.80
0.9 msec	0.77
1.0 msec	0.75
1.1 msec	0.75
1.2 msec	0.77
1.3 msec	0.80
1.4 msec	0.83
1.5 msec	0.83
(1.0 msec	0.72)*
1.6 msec	0.84
2.0 msec	0.85
3.0 msec	1.07

*Duplicate run of 1.0 msec delay following change in solution.

considerably higher values of B%P in these experiments are reasonable when one considers that the peak height is proportional to the concentration while the baseline should be basically unchanged.

As in the two experiments using higher concentration solutions, these experiments indicated a minimum occurring at a time much shorter than 40 msec. In the case of the more dilute solution, the minimum of B%P in fact occurred at a shorter delay time than for the higher concentration solution. In this case the optimum delay time was found to be approximately 0.7 msec, and if standard error is considered the minimum occurred in the span of 0.7 to 0.9 msec. The reason for the

optimum signal-to-noise ratio occurring at a shorter delay time is not apparent.

In summation, the data from this study indicate that shorter delay times than are presently being used in commercial instruments can, in fact, be used without complication due to the presence of the capacitance current. While the data indicate that the optimum time is in the neighborhood of 1 msec, further investigations need to be made for solutions where the electroactive species are in still lower concentrations. However, such studies will require the addition of a gated integrator to the instrument in order to more effectively filter noise.

Effect of Positive Feedback on B%P and Delay Time

It was expected from the theory in Chapter I that the application of positive feedback would result in faster potentiostat rise time. This faster rise time would then result in a faster decay of the capacitance current due to the lower effective rc product. Based on this reasoning it was expected that by proper application of positive feedback to the potentiostat, at any given time the capacitance current should be lower when feedback was applied than when it was not. This theory seems to be proven by the data in Table 5.

In this study a solution similar to the standard solution was used except that the supporting electrolyte concentration was 0.01 F instead of 0.1 F. It can be seen from the data that the minimum B%P for both feedback and non-feedback occurred at about 1.0 msec, but that the run which incorporated the feedback showed a 21 percent

Table 5. Effect of Positive Feedback.

No Feedback					
Delay Time	Left Base	Peak	Right Base	Total Base	Base % Peak
0.3	31,115 ± 4,575	506,880	16,806 ± 3,422	23,891 ± 8,970	4.71
0.4	24,240 ± 3,736	514,048	15,980 ± 2,254	20,292 ± 4,993	3.94
0.6	10,597 ± 5,013	493,056	8,179 ± 2,790	8,639 ± 2,560	1.75
0.8	10,592 ± 3,057	483,584	6,654 ± 3,531	8,947 ± 3,882	1.85
1.0	9,522 ± 5,029	459,008	4,294 ± 1,118	6,787 ± 4,493	1.47
2.0	7,019 ± 2,570	427,776	6,014 ± 2,343	6,546 ± 2,586	1.53
6.0	6,239 ± 2,678	312,064	4,734 ± 824	5,491 ± 2,097	1.75
Feedback					
Delay Time	Left Base	Peak	Right Base	Total Base	Base % Peak
0.3	12,378 ± 2,648	701,440	10,112 ± 3,844	11,042 ± 3,219	1.57
0.4	9,558 ± 3,528	683,520	7,753 ± 3,057	8,917 ± 3,368	1.30
0.6	8,813 ± 4,011	632,832	9,053 ± 3,241	8,704 ± 3,407	1.37
0.8	7,714 ± 2,529	615,424	8,593 ± 6,044	8,023 ± 4,766	1.30
1.0	6,668 ± 1,360	606,208	7,488 ± 3,170	7,057 ± 2,557	1.16
2.0	7,223 ± 2,184	522,752	6,768 ± 2,851	6,906 ± 2,606	1.32
6.0	7,763 ± 3,813	368,128	7,277 ± 5,193	7,950 ± 4,481	1.21

improvement of B%P over the non-feedback run. This improvement indicates that the capacitance current has been reduced considerably. In addition to the B%P being considerably reduced it should be noted that the left-hand baselines in the non-feedback runs are higher in relation to the righthand baselines than in the feedback runs. This relationship of lefthand baselines to righthand baselines is attributable to the presence of capacitance current since the differential double-layer capacitance is greater to the left of the cadmium peak.

Another interesting fact is indicated by the data in Table 5. From the peak data of each run it can be seen that in the presence of feedback the heights of the peaks are greater than in the non-feedback cases. This difference is thought to be due to the fact that in the non-feedback cases the Faradaic current is hidden in the capacitance current, and thus the Faradaic peak appears to be considerably lower. Therefore the use of positive feedback allows one to minimize the capacitance current and thus increase the sensitivity of the method toward the electroactive species.

In conclusion it can be seen that by the use of a properly designed positive feedback circuit the capacitance current can be rejected at a shorter time than otherwise possible.

Effect of Drop Size

It is the contention of other experimenters that as the drop time of the DME decreases, allowing a shorter analysis time, the sensitivity towards the electroactive species decreases. This effect, if it exists, is dependent on the drop size. In order to investigate the

effect of drop size, experiments were performed by varying the time at which pulses were initiated. The first experimental set of runs utilized only one pulse per drop, or in effect pulse polarography, while the second set used four pulses per drop, a form of square-wave polarography. As can be seen from both Figures 9 and 10 and Tables 6 and 7, the B%P decreases steadily as the time in the drop life at which the pulse(s) were applied increases. This decrease in B%P with the increasing time in the drop, hence increasing drop size, is in effect an increase in sensitivity towards the electroactive species. While a plot of B%P exhibits a concave curve with increasing time, peak height versus time of pulse application appears to be linear, at least in the range of interest. Based on the data found in the pulse polarography experiment, every second decrease in drop time was at a cost of 15.6 percent in peak height. The results from the square-wave experiment indicate a 16.1 per cent decrease in peak height for each second in pulse application. Based on these two experiments it is seen that a trade-off must be applied between short times of analysis and sensitivity. In the cases where polarography is used for trace analysis, the experimenter is advised to use the longest pulse application time feasible.

Noise Averaging

The purpose of these experiments was to investigate two different modes of noise averaging which could be used in square-wave polarography. In the first experiment a series of runs were made to determine the effect of noise averaging in relation to the number of square waves applied during the drop life. The second experiment

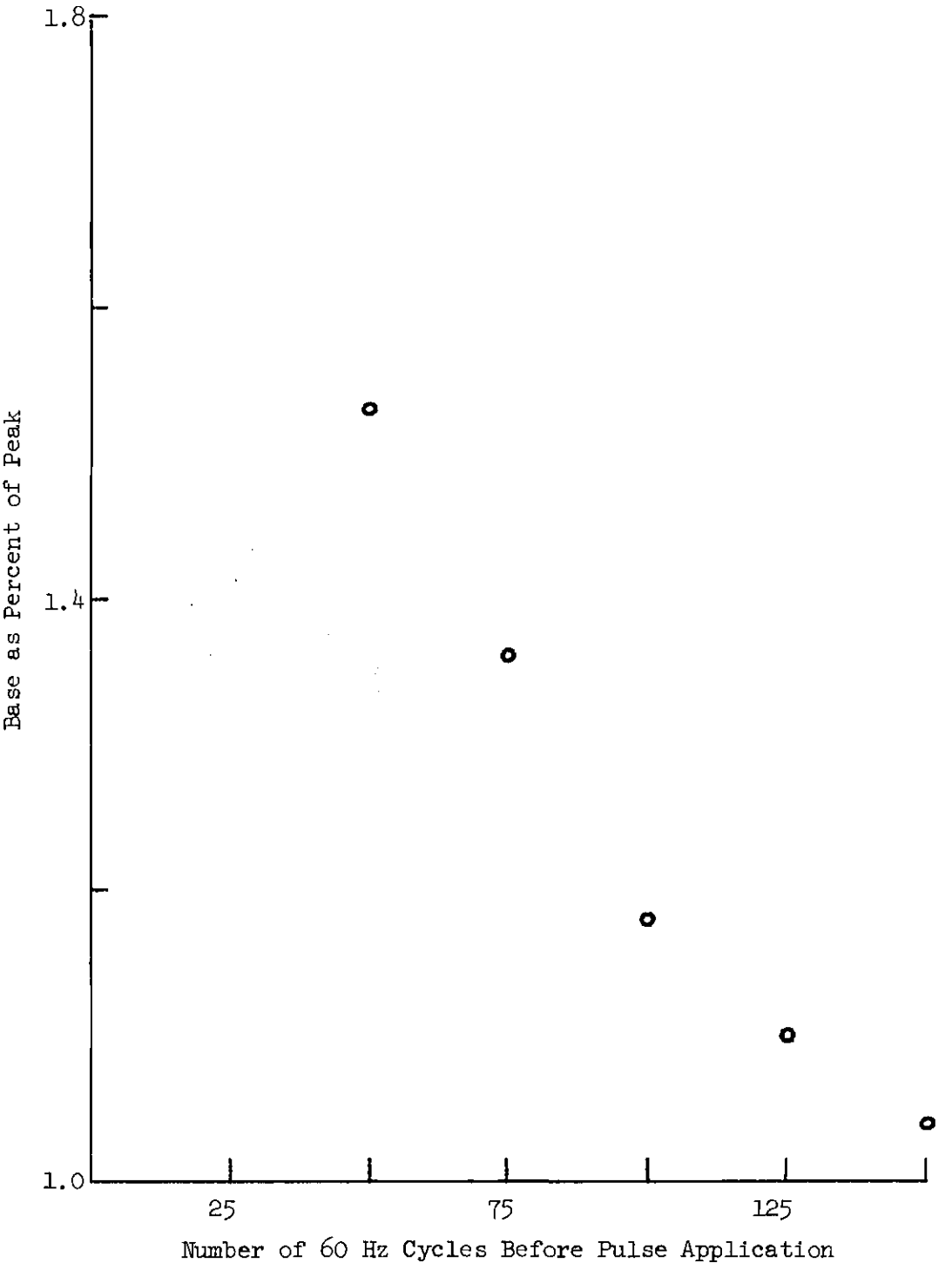

Figure 9. Base Percent Peak versus Time in Drop Life. Single Pulse.

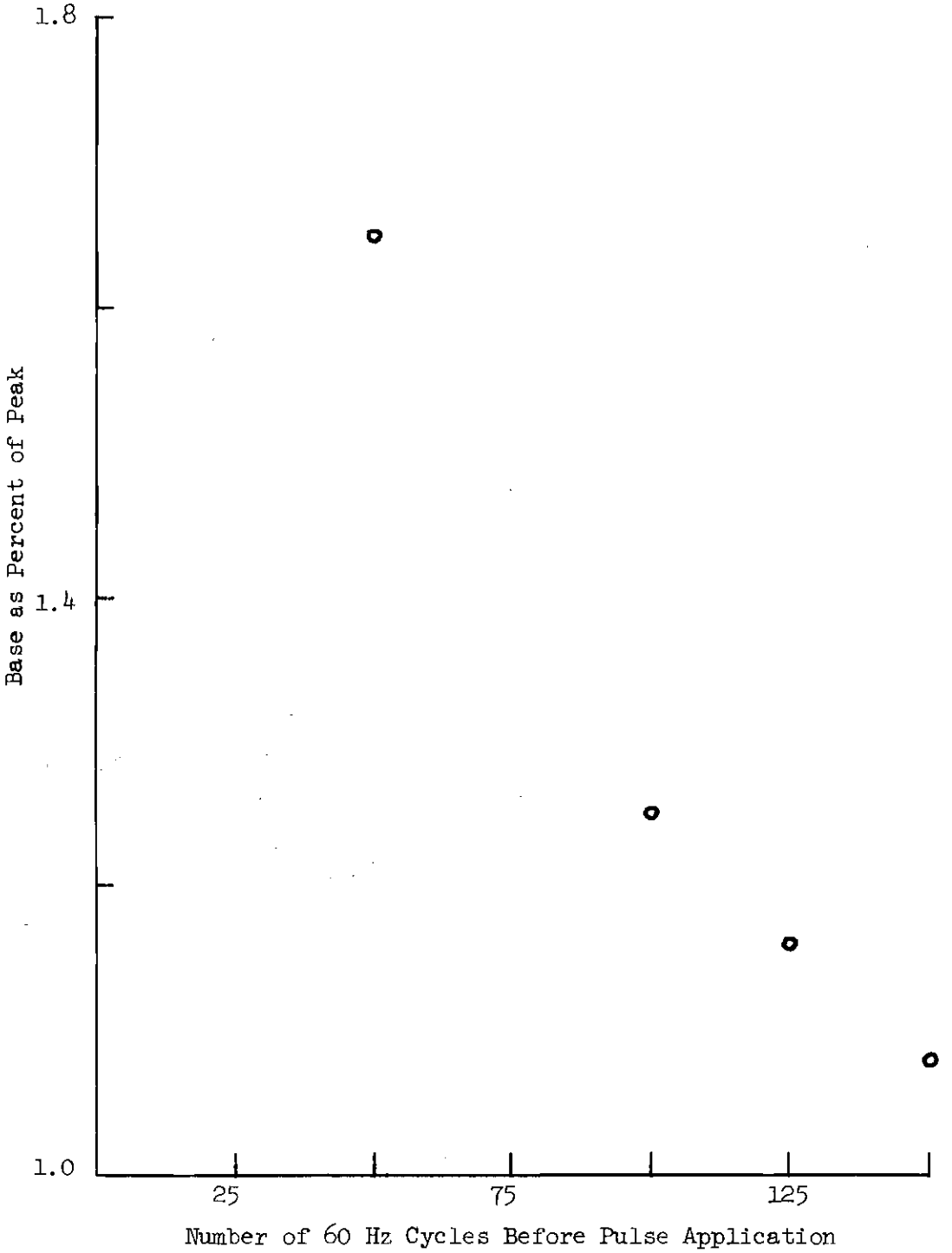

Figure 10. Base Percent Peak versus Time in Drop Life. Four Pulses.

Table 6. Current Versus Drop Time (One Pulse).

Number of 60 Hz Cycles	Delay Before Pulse Application (sec)	B%P
150	5.00	1.04
125	4.17	1.10
100	3.33	1.19
75	2.50	1.36
50	1.67	1.53

Note: 3.33 sec delay average of 2 runs all others are a single run.

Table 7. Current Versus Drop Time (Four Pulses).

Number of 60 Hz Cycles	Delay Before Pulse Application (sec)	B%P
150	5.00	1.08[a]
125	4.17	1.15[b]
100	3.33	1.26[b]
50	1.67	1.64[c]

a) Average of 1 run
b) Average of 2 runs
c) Average of 3 runs

investigated the noise averaging which took place during each square-wave cycle. By investigating both parameters it was hoped that a better understanding, as to the best design for a hard-wired instrument, could be obtained.

For the first experiment, it was decided to have the computer acquire 100 data points per square-wave cycle. By then increasing the number of square-wave cycles taken on a particular drop, the effect of increasing the number of square-waves per drop could be determined. To minimize all other effects, the spacing between each discrete current value was constant and the delay time before the first current value was held constant at 1.0 msec.

For this experiment, unlike the preceding experiments, the graph (Figure 11) plots the number of cycles versus the standard deviation of the baseline, rather than B%P. As can be seen in Figure 11 and Table 8, the normalized standard deviation of the baseline dropped from 25.24 units to 19.32 units upon doubling the number of cycles, and therefore the number of discrete points, taken. When the number of cycles was again doubled (to 4 cycles per drop) the standard deviation of the baseline continued to drop to 18.08 units. This continued to the point where 50 square-wave cycles were applied to each drop (with an aggregate total of 5000 discrete points), and the standard deviation of the baseline dropped to 16.97 units. From this experiment it can be seen that by using multiple square-waves per drop a much better noise everaging can be achieved than with a single square-wave, or pulse polarography.

The second noise-averaging experiment was to determine the effect

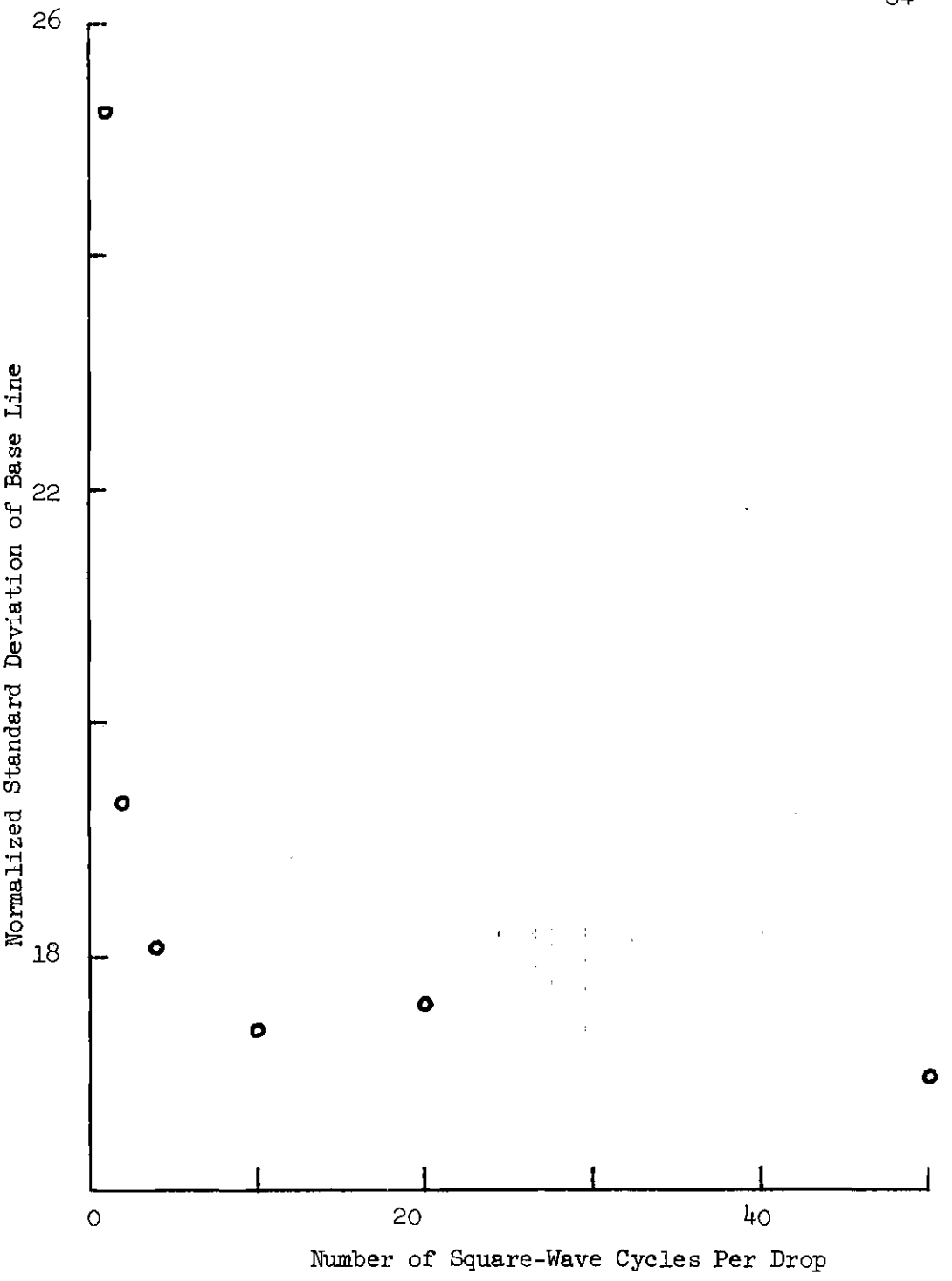

Figure 11. Reduction of Noise by Increasing Number of Data Points.

Table 8. Effect of Number of Cycles on Noise Reduction.

Cycles/Drop	Σ Values Obtained	Normalized Standard Deviation
1	100	25.24
2	200	19.32
4	400	18.08
10	1000	17.37
20	2000	17.59
50	5000	16.97

of the number of discrete data points taken per square-wave cycle. In this case the total number of discrete values was held to a constant 100 by varying inversely the number of discrete data points per cycle versus the number of cycles per drop. To illustrate, when 100 discrete points were taken per square-wave cycle, only one square-wave cycle was applied per drop, but when 50 discrete data points were taken per square wave then two cycles were applied per drop thus holding the discrete points to 100. This discrete approach was adopted to avoid the problem of insufficient data points for statistical analysis. An alternative to this would have been to increase the number of polarograms as the number of points per cycle was decreased.

Upon studying the data presented in Figure 12 and Table 9, it can be seen that as the number of discrete values per cycle increased, the standard deviation of the baseline dropped off remarkably. Even in the case of 100 discrete points per cycle, and one cycle per drop, the standard deviation was still well above that found when multiple cycles were used, each utilizing 100 discrete points.

Thus baseline noise is reduced by increasing the number of data points per cycle as well as by increasing the number of square-wave cycles. These results also indicate that square-wave polarography utilizing a gated integrator should be less affected by noise, and therefore more sensitive, than either pulse polarography or square-wave polarography as it is usually practiced.

It is also clear from the experiments that the number of cycles and the number of points taken per cycle have no affect on the peak half-width or the location of the potential axis.

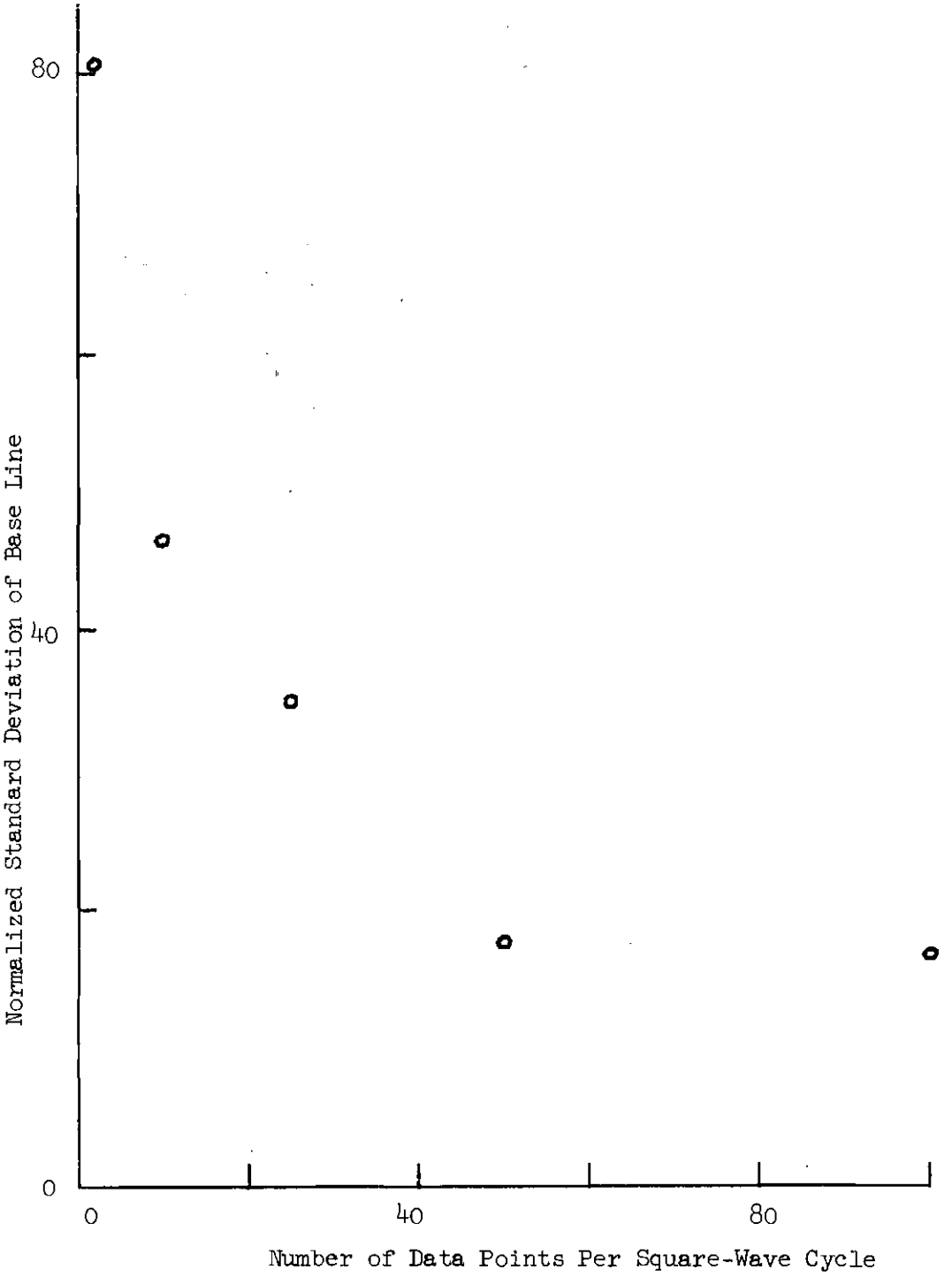

Figure 12. Reduction of Noise by Increasing Number of Data Points Per Square-Wave Cycle.

Table 9. Effect of Number of Current Values Per Cycle on Noise Reduction.

Cycles/Drop	Values/Cycle	Standard Deviation
1	100	16.74
2	50	17.62
4	25	34.84
10	10	46.55
50	2	80.69

The data of Table 9 were obtained approximately a week after the data of Table 8. In the interim time, several changes were made in the grounding system of the instrument in an attempt to lower the noise level. As a result, the first point of Table 9 is 16.74 as compared to 25.24 in Table 8 although the experiments were nominally repeats. This is an example of the day to day changes in the noise environment that would have made the results of this study meaningless had not the procedure been adopted to run complete series of experiments in as short a time as possible. To repeat, the trends indicated by the data in Tables 8 and 9 are valid. However, no special significance should be attached to the exact numerical values from either series of experiments.

Miscellaneous Experiments

As with most studies, there were a few experiments which did not fit into a neat category. A discussion of these experiments is found below.

One of the concerns when dealing with a combination of analog and digital instrumentation is the introduction of artifacts due to the interface and not due to the experiment in question. An experiment was made to identify the relationship of B%P to the effective number of ADC levels utilized at a particular analog amplification. In this experiment reference is made to the parameter "P_e". This parameter is found by dividing the actual peak height by the number of samples added together to determine the peak height. This then makes P_e the maximum number of ADC levels used for a particular run. Figure 13 and Table 10 reflect the results of this experiment. The "●" symbols on the graph

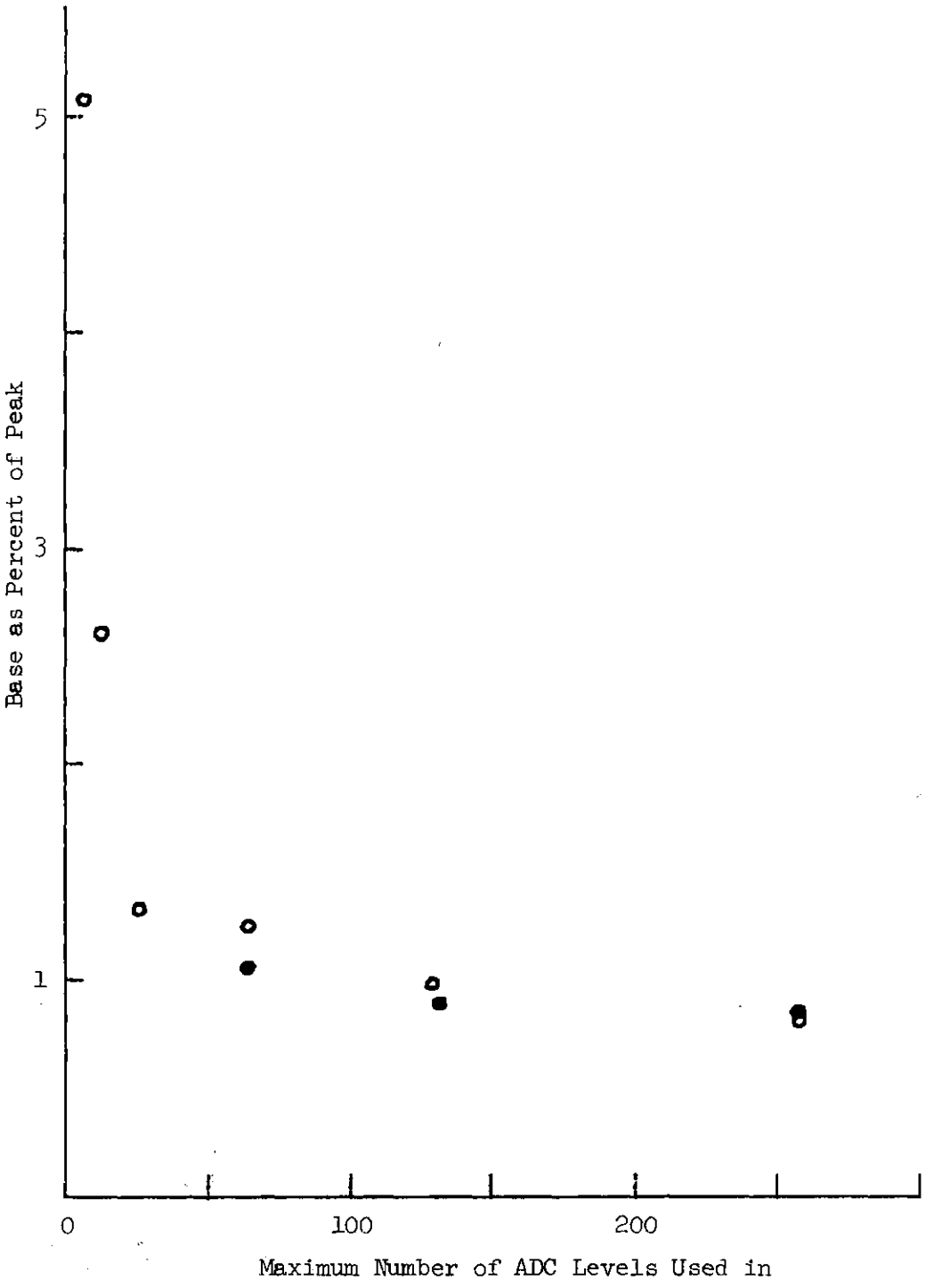

Figure 13. Base Percent Peak versus Number of ADC Levels.
o, First Stage Amplification = 1 milliamp/volt
●, First Stage Amplification = 0.1 milliamp/volt

Table 10. Relationship of Number of ADC Levels to Noise.

1st Stage Amp	P_E	B%P
1 ma/v	6.6	5.08
1 ma/v	13.0	2.60
1 ma/v	26.2	1.33
1 ma/v	64.3	1.25
1 ma/v	128.9	0.98
1 ma/v	257.6	0.81
0.1 ma/v	64.2	1.06
0.1 ma/v	131.5	0.89
0.1 ma/v	257.2	0.85
0.1 ma/v	626.3	1.02

represent a first stage amplification of 1 ma/v while the "o" indicate a first stage amplification of 0.1 ma/v. From the graph it can be seen that when P_e is very small the B%P was quite high, and as more and more levels of ADC are utilized the B%P rapidly drops off to approach a limit of about 0.80 to 0.85 B%P. This result is reasonable when one realizes that in the cases where P_e is small, the baseline would activate either zero levels or one level with the result that the apparent noise is higher than it is really. As more levels are employed the normal noise activates relatively fewer ADC levels above the mean value of the baseline and B%P drops. This results in the observation that once the peak values activate at least seven bits of the ADC the signal-to-noise ratio, as represented by B%P, remains approximately constant and can be ignored safely. As a result of these findings all the experiments utilized analog amplifier settings which resulted in P_e values around 256. The B%P value for an amplifier setting of 0.1 ma/v (see Table 10) showed an upward turn. The explanation here was that the peak values during this run were occasionally saturating the ADC levels resulting in a truncated peak value, and as the baseline values did not observe such truncation and remained active, the effect was an increase in B%P. The final determination of these experiments indicated again that as long as the peak values utilized approximately seven ADC levels and did not saturate the ADC the interface resulted in very little variation in B%P.

An experiment was run to determine the change in peak width with increases in pulse height. Theory predicts that the peak width should be 89.4/n millivolts under conditions where Equation 1 holds and

progressively wider when Equation 2 is necessary (See Chapter I). As can be seen in Table 11 the peak widths for the first two pulse sizes

Table 11. Experimental Relationship of Pulse Size to Peak Width.

Pulse Size	Peak Width
10	44
20	44
40	54.7
80	78.1

were well within measurement error of the answers predicted by either Equation 1 or Equation 2. As the pulse size increased, and Equation 1 no longer held, the peak width increased as predicted from Equation 2. These results have been taken to indicate that the program which was used in this work was working properly.

Summary

As the experiments have shown, the use of a combined analog and digital polarographic system has resulted in some decisive conclusions. The delay time experiments proved that delay times of a much shorter duration than are presently being used are possible and in fact desirable. Further, by the use of positive feedback to give faster rise times, it should be possible to continue to use short delay times at lower concentrations of supporting electrolyte. By the use of specifically designed analog instruments and the use of gated integrators,

perhaps with the output of the integrator connected to a digital computer, it should be possible to utilize these short delay times at lower and lower concentrations. The final conclusion of interest is the decrease in signal-to-noise ratios which can be accomplished by the use of multiple square-wave applications versus a single square-wave, or pulse polarography as is commonly used today.

The work done was not meant as a panacea for all the present ills of instrumentation: rather it attempted to show the feasibility not only of the concepts studied and proven, but also of utilizing a combined analog-digital instrument to explore quickly new concepts and ideas. The author believes that the best instruments in the near future will utilize analog control circuitry with data handling being done with digital computers. The hybrid digital-analog instrument allows remarkable versatility where new parameters are to be reviewed before building inflexible analog circuits.

APPENDIX A

The conditions used in the check were as follows:

	TTY Input	Meaning
Initial Potential	4500	- 0.32 V
Step Size	42	- 40 mV pulse
Ramp Step Size	4	- 4 mV ramp step
Number of Drops	90	90 drops
Clock #1	0 & 0014	enable ST #4
Clock #2	10 & 5450	1 msec delay to 1st point
Clock #3	1 & 5440	0.1 msec between points
Wait	150	150 cycles of 60 Hz
Cycles per Drop	50	50 cycles of square wave/drop
Multiple Values	50	50 points/cycle
Amplifiers	3 - 3	1 V output = 40 μa cell current
Damping Filters	1 - 2	
Feedback	0	

LITERATURE CITED*

1. Heyrovsky, J., Chem Listy, 16, 256, (1922).

2. Ilkovic, D., Coll. Czech. Chem. Commun., 6, 498, (1934).

3. Liddle, J. A., "A Study of Electroanalytical Methods Employing Potential Step Perturbation and the Investigation of the Kinetic Parameters of the Polarographic Reduction of Hydrated Zinc Ions in Potassium Nitrate", Ph.D. Thesis, Georgia Institute of Technology, Atlanta, Georgia, (March 1972).

4. Barker, G. C., and I. Jenkins, Analyst, 77, 685, (1952).

5. Barker, G. C., AERE, C/R 1563, (1957).

6. Parry, E. P., and R. A. Osteryoung, Anal. Chem., 37, 1634, (1965).

7. Carter, R. J., Private Communication.

8. Christie, J. H., and R. A. Osteryoung, Electroanal. Chem., 49, 30, (1974).

9. Sturrock, P. E., and R. J. Carter, Crit. Rev. Anal. Chem., 5, 201, (1975).

10. Barker, G. C., and A. W. Gardner, Z. Anal. Chem., 179, 79, (1960).

11. Brown, E. R., and D. E. Smith, Anal. Chem., 40, 1411, (1968).

12. Christie, J. H., Private Communication.

13. Digital Equipment Corporation, Maynard, Massachusetts.
    a. Symbolic Editor, DEC-08-ESCA-PB, (1970)
    b. PAL III, DEC-08-ASC1-PB, (1970)
    c. ODT, DEC-08-COC1-PB, (1967)

14. Digital Equipment Corporation Users Society, Maynard, Massachusetts, Program 8-149.

*Journal title abbreviations used are listed in "Index of Periodicals," Chemical Abstracts, (1970).

VITA

Alan Conrad Hayman was born 19 November 1947, in Wilmington, Delaware, to Jackson L. Hayman and Marjorie C. Hayman. He attended Buchtel Senior High School in Akron, Ohio and graduated in June 1965. In September 1965 he entered the University of Delaware in Newark, Delaware, where he received a B.S. degree in chemistry in June of 1969.

In August 1969 he was married to Katherine Joslyn Niederriter of Philadelphia, Pennsylvania.

In September 1969 he entered Georgia Institute of Technology and was appointed as a Graduate Teaching Assistant. In March 1975 he accepted a position as Analytical Chemist for Union Carbide Corporation in South Charleston, West Virginia.